2-Hydroxymethyl-18-crown-6 as an efficient organocatalyst for α - aminophosphonates synthesized under eco-friendly conditions, DFT, molecular docking and ADME/T studies

Samia Guezane-Lakoud, Meriem Ferrah, Mounia Merabet-Khelassi, Nourhane Touil, Martial Toffano, Louisa Aribi-Zouioueche

Article Information

Article Type:	research-article
Journal Title:	Journal of Biomolecular Structure and Dynamics
Publisher:	Taylor & Francis
DOI Number:	10.1080/07391102.2023.2213336
Volume Number:	0
Issue Number:	0
First Page:	1
Last Page:	17
Copyright:	© 2023 Informa UK Limited, trading as Taylor & Francis Group
Received Date:	2023-2-17
Accepted Date:	2023-5-4

2-Hydroxymethyl-18-crown-6 as an efficient organocatalyst for α-aminophosphonates synthesized under eco-friendly conditions, DFT, molecular docking and ADME/T studies

Left running head: G.-L. SAMIA ET AL.

Short title : Journal of Biomolecular Structure and Dynamics

AQ0

Samia Guezane-Lakoud[a], Meriem Ferrah[a], Mounia Merabet-Khelassi[a], Nourhane Touil[a], Martial Toffano[b] and Louisa Aribi-Zouioueche[a] AQ1

[a]Ecocompatible Asymmetric Catalysis Laboratory (LCAE) Badji Mokhtar Annaba-University, Annaba, Algeria;

[b]Equipe de Catalyse Moléculaire-ICMMO Bât 420. Université Paris-Saclay, Paris, France AQ2

Footnotes

Supplemental data for this article can be accessed online at https://doi.org/10.1080/07391102.2023.2213336.

Corresponding Author

CONTACT Guezane-Lakoud Samia samia.guezanelakoud@univ-annaba.dz

Abstract

Eco-friendly and simple procedure has been developed for the synthesis of α-aminophosphonates that act as topoisomerase II α-inhibiting anticancer agent, using 2-hydroxymethyl-18-crown-6 as an unexpected homogeneous organocatalyst in multicomponents reaction of aromatic aldehyde, aniline and diethylphosphite in one pot *via Kabachnik–Fields* reaction. This efficient method proceeds with catalytic amount, transition metal-free, at room temperature within short reaction time, giving the α-aminophosphonates derivatives **(4a–r)** in high chemical yields (up to 80%). Theoretical DFT calculations of three compounds **(4p, 4q** and **4r)** were carried out in a gas phase at CAM-B3LYP 6-31G (d,p) basis set to predict the molecular geometries and chemical reactivity descriptors. The frontier orbital energies (HOMO/LUMO) were described the charge transfer and used to predict structure-activity relationship study. Molecular electrostatic potential (MEP) has also been analyzed. Molecular docking studies are implemented to analyze the binding energy and compared with Adriamycin against 1ZXM receptor which to be considered as antitumor candidates. *In silico* pharmacological ADMET properties as Drug likeness and oral activity have been carried out based on Lipinski's rule of five.

Communicated by Ramaswamy H. Sarma

KEYWORDS

α-Aminophosphonates; crown ether; *Kabachnik–Fields* reaction; DFT; molecular docking; ADMET prediction

Note: Any change made here needs to be made in the corresponding section at the end of the article.

The author(s) reported there is no funding associated with the work featured in this article. AQ6

1. Introduction

Among the types of phosphonates derivatives, systems containing nitrogen, oxygen and phosphore atoms have the most biological and biochemical aspects (Mucha et al., 2011; Schug & Lindner, 2005). Considerable attention is continuously devoted to α-aminophosphonates because of analogy with amino acid. These compounds exhibit significant biological and pharmacological activities, they are employed as enzyme inhibitor (Grzywa & Sieńczyk, 2013; Maier, 1990), cholinesterase inhibitors (Uparkar et al., 2022), inhibitors of UDP-galactopyranose mutase, also as antitumor agents (Pan et al., 2007), and growth inhibition on *Paramecium* sp. (Guezane-Lakoud et al., 2015). In agrochemistry, a number of α-aminophosphonates derivatives are used as fungicidal and herbicidal agents (Bonarska et al., 2002; Maier & Diel, 1991). Due to their outstanding properties, the construction of α-aminophosphonates compounds remains an important and demanding topic in chemical synthesis. Various approaches were described to synthesize their derivatives *via Kabachnik–Fields* reaction using *Lewis* and *Brønsted* acids (Aissa et al., 2022; Lakoud et al., 2016; Laschat & Kunz, 1992; Sivala et al., 2016; Yadav et al., 2001), lipase (Aissa et al., 2019; Guezane-Lakoud et al., 2017), oxalic acid (Vahda et al., 2008) ionic liquid (Rostamnia & Amini, 2014), organocatalyst (Aissa et al., 2021; Ferrah et al., 2022), heteropolyacids (Heydari et al., 2007) and *β*-cyclodextrin (Rostamnia & Doustkhah, 2015). However, the catalytic process suffers many drawbacks, such as the use of the high temperature, long reaction times, metal-catalyst, drastic reaction conditions, stoichiometric amount of catalyst and tedious workup of the purification. There is still a strong demand for new efficient and easy methods to reduce the difficulties for the synthesis of α-aminophosphonates. Herein, we envisioned the use of the crown ether as a new type of organocatalyst for the multicomponent *Kabachnik–Fields* reaction. Crown ethers represent, from its discovery by *Liittringhaus'* in 1937

(Liittringhaus, 1937), then by *Pedersen* in 1967 for the formation of stable complexes with salts of alkali and alkaline earth metals (Pedersen, 1967), a great interest as structure-specific in many areas of science. Crown ethers include as 'host-guest' due to the presence of a hydrophobic ring surrounding a hydrophilic cavity leading to the complex formation with metal ions (Dix et al., 1980; Pedersen, 1970). Some of the first uses of crown ethers were as solvent extraction reagents (Mcdowell, 1988), phase transfer catalysis (Cinquini & Tundo, 1976), and they have a property of ion-transport and form complexes with specific ions, particularly of sodium and potassium ions and facilitate their transport across cell membranes (Lamb et al., 1981), also they have been used as additive to improve the reactivity and selectivity of some lipases (Merabet et al., 2007).Chiral crown ethers have been also used in asymmetric chemistry as chiral selectors and reported the separation of amino acids and drug enantiomers (Hyun, 2012). On the other hand, crown ethers are numerously used as catalysts by noncovalent binding with the organic neutral and ionic species to promote various reactions such as aldolization (Nagayama & Kobayashi, 2000), *Michael* reaction (Pham et al., 2011), allylic substitution and asymmetric hydrogenation (Luo et al., 2020). In addition, the introduction of amine-substituted by crown ether as a reagent has been reported to produce α-aminophosphonates based on the combination of radiation-induced graft polymerization (Omichi et al., 2019). Herein, we have evaluated for the first time the use of crown ether as an efficient homogeneous organocatalyst for the synthesis of various α-aminophosphonates from aromatic aldehydes, anilines and diethylphosphite *via* multicomponents reaction under mild conditions. On the other hand, the DFT study, in *silico* molecular docking and ADMET prediction of various derivatives of α-aminophosphonates have been widely described (Aita et al., 2021; Kerkour et al., 2023; Mirzaei et al., 2018). In this context, we have carried out the prediction of molecular geometry parameters, HOMO-LUMO orbitals, intramolecular charge transfer and molecular electrostatic potential in CAM-B3LYP/6-31G (d,p) level of theory to investigate the physicochemical properties of the characterized structure of **4p**, **4q** and **4r** as target molecules. As mentioned above, α-aminophosphonates have antitumoral activities. The 1ZXM protein was chosen for molecular docking studies in order to predict the potential 1ZXM binding affinity and binding interactions of the examined compounds. Pharmacological ADMET properties as Drug likeness of the compounds were assessed based on Lipinski's rule of five.

2. Materials and methods

2.1. Chemistry

All reagents were purchased from Sigma-Aldrich or Acros Company used without further purification. Reactions were monitored by thin layer chromatography (TLC) carried out on 0.25-mm Merck silica gel plates (60F-254) using ultraviolet light (254 nm) as the visualizing agent and $KMnO_4$ solution as developing agents. NMR spectra were recorded with Bruker spectrometers operating at (360, 300 and 250 MHz for 1H, 90, 75 or 63 MHz for ^{13}C and 101 MHz or 121 MHz for ^{31}P). Chemical shift of Solvent reference peaks used were $CDCl_3$ (δ = 7.26 ppm) for 1H and (δ = 77 ppm) for ^{13}C NMR spectra, while H_3PO_4 was used as external standard for chemical shift references for ^{31}P NMR. Couplings constants (*J*) are given in Hz, with the Following abbreviations multiplicity: s = singlet, d = doublet, t = triplet, q = quartet, m = multiplet, br = broad signal. Mass spectra were taken by a MicrOTOF-Q Bruker spectrometer using electrospray ionization (ESI) analysis. Melting points were measured using Buchi Melting Point B-545.

2.2. General experimental procedure for the synthesis of diethyl phenyl α-aminophosphonates 4a–r

To the reaction mixture containing aromatic aldehyde (101.12 mg, 1 mmol), aniline (93 mg, 1 mmol) and diethylphosphite (165 mg, 1.2 mmol) in THF (2 mL), 2-hydroxymethyl-18-crown ether-6 (5 mol%) was added, it was stirred within 15 min at room temperature. The reaction progress was monitored by TLC. The mixture was extracted with dichloromethane (10 mL × 2). The organic phases were combined and evaporated in vacuum. The crude product was purified by crystallization in hexane to afford the α-aminophosphonates derivatives 4a-r with good to excellent chemical yields.

2.2.1. Diethyl [phenyl (phenylamino) methyl] phosphonate (4a)

White crystalline solid, 91% yield, mp 88 °C. ^1H NMR (250 MHz, $CDCl_3$, 25 °C) δ 7.52–7.29 (m, 6H, HAr), 7.16–7.10 (t, 1H, *J* = 7.9 Hz, HAr), 6.75–6.69 (t, 1H, *J* = 7.3 Hz, HAr), 6.64–6.61 (m, 2H, HAr), 4.84–4.75 (d, 1H, J_{HP} = 24.3 Hz, CHP), 4.18–4.10 (2H, m, $–OCH_2–CH_3$), 4.01–3.76 (2H, m, $–OCH_2–CH_3$), 3.74–3.63 (1H, m, $–OCH_2–CH_3$), 1.31 (t, 3H, *J* = 7.1 Hz, $–OCH_2–CH_3$), 1.14 (t, 3H, *J* = 7.1 Hz, $–OCH_2– CH_3$). ^{13}C NMR (63 MHz, $CDCl_3$, 25 °C): δ 146.33 (d, *J* = 14.5 Hz); 136.00, 129.29, 128.74, 128.71, 128.00, 127.03, 118.40, 113.87, 63.27 (d, J^2 CP = 6.9 Hz), 57.29, 54.90, 16.46 (d, J^3_{CP} = 15.1), 16.37 (d, J^3_{CP} = 5.6 Hz). ^{31}P NMR (101 MHz, $CDCl_3$, 25 °C) δ 22.46 ppm. HRMS (ESI) *m/z* calcd for $C_{17}H_{23}NO_3P$ [M + H^+]: 320.1408; Found 320.141.

2.2.2. Diethyl [4-chlorophenyl (phenylamino) methyl] phosphonate (4b)

White crystalline solid, 80% yield, mp: 86.8 °C. ^{1} HNMR (300 MHz, $CDCl_3$, 25 °C) δ 7.44 (dd, *J* = 8.6, 2.3 Hz, 2H, HAr), 7.21–7.38 (m, 2H, HAr), 7.13 (dd, *J* = 8.5, 7.4 Hz, 2H, HAr), 6.73 (t, 1H, *J* = 7.4 Hz, HAr), 6.58 (dd, 2H, *J* = 8.6, 0.9 Hz, HAr), 4.75 (d, 1H, J_{HP} = 24.5 Hz, CHP), 4.05–4.21 (m, 2H, $–OCH_2–CH_3$), 3.92–4.06 (m, 1H, $–OCH_2–CH_3$), 3.75–3.80 (m, 1H, $–OCH_2–CH_3$), 1.30 (t, 3H, *J* = 7.0 Hz, $–OCH_2–CH_3$), 1.18 (t, 3H, *J* = 7.0 Hz, $–OCH_2–CH_3$), ^{13}CNMR (75 MHz, $CDCl_3$, 25 °C) δ 146.01 (d, *J* = 14.6 Hz), 134.60, 133.70, 129.26 128.19, 128.89, 128.86, 118.66, 113.83, 63.38 (d, J^2=6.8 Hz), 56.60, 54.61, 30.94, 16.36 (d, J^3_{CP}=13.7 Hz), 16.36 (d, J^3_{CP}=5.7 Hz). ^{31}P NMR (121 MHz, $CDCl_3$, 25 °C) δ 23.24 ppm.

2.2.3. Diethyl [4-nitrophenyl (phenylamino) methyl] phosphonate (4c)

Yellow crystalline solid, 93% yield, mp 89.2 °C. ^1H NMR (250 MHz, $CDCl_3$, 25 °C) δ 8.22–8.19 (m, 2H, HAr), 7.69–7.64 (dd, 2H, J_{HP} = 8.80, 2.3 Hz, HAr), 7. 15–7. 09 (m, 2H, HAr), 6.77–6.71 (t, 2H, *J* = 7.4 Hz, HAr), 6.59–6.52 (m, 2H, HAr), 4.92–4.81 (d, 1H, J_{HP} = 25.2 Hz, CHP), 4.19–4.10 (m, 2H, $–OCH_2–CH_3$), 4.09–4.02 (m, 1H, $–OCH_2–CH_3$), 3. 99–3. 95 (m, 1H, $–OCH_2–CH_3$), 1.30 (t, 3H, *J* = 7.00 Hz, $–OCH_2–CH_3$), 1.19 (t, 3H, *J* = 7.1 Hz, $–OCH_2–CH_3$). ^{13}C NMR (63 MHz, $CDCl_3$, 25 °C) δ 147.59, 145.63 (d, *J* = 14.2 Hz), 144.04 (d, *J* = 2.5 Hz), 129.34, 128.63 (d, *J* = 4.9 Hz), 123.75, 119.10, 113.79, 63.60 (dd, J^2= 17.1, 6.9 Hz), 57.20, 54.84, 16.30 (dd, J^3_{CP} = 10.3, 5.5 Hz). ^{31}P NMR (101 MHz, $CDCl_3$, 25 °C): δ 21.31 ppm. HRMS (ESI) *m/z* calcd for $C_{17}H_{21}N_2O_5P$ [M + H^+]: 387.1094; Found 387.1080.

2.2.4. Diethyl [1-naphtyl (phenylamino) methyl] phosphonate (4d)

White crystalline solid, 88% yield; mp 123 °C. ^{1}H NMR (250 MHz, $CDCl_3$, 25 °C) δ 8.26 (d, 1H, J_{HP} = 8.3 Hz, HAr), 7.89–7.44 (m, 6H, HAr), 7.05–7.02 (dd, 2H, *J* = 8.5, 7.4 Hz, HAr), 6.68–6.63 (dd, 1H, *J* = 10.6, 4.1 Hz, HAr), 6.57–6.53 (m, 2H, HAr), 5.60 (d, 1H, J_{HP} = 24.1 Hz, CHP), 5.10 (s, 1H, NH), 4.25–4.13 (m, 2H, –OCH_2–CH_3), 3.75–3.72 (m, 1H, –OCH_2–CH_3), 3.25–3.15 (m, 1H, –OCH_2–CH_3), 1.33 (t, 3H, *J* = 7.00 Hz, –OCH_2–CH_3), 0.70 (t, 3H, *J* = 7.1 Hz, –OCH_2–CH_3). ^{13}C NMR (63 MHz, $CDCl_3$, 25 °C) δ 146.11 (d, *J* = 13.9 Hz), 133.81, 131.63 (d, *J* = 8.0 Hz), 129.09 (d, *J* = 10.6 Hz), 128.44, 126.25, 126.05, 125.65, 125.37 (d, *J* = 5.8 Hz), 122.94, 118.26, 113.57, 63.26 (dd, J^2_{CP} = 12.4, 6.8 Hz), 52.67, 50.25, 16.45 (d, J^3_{CP} = 6.2 Hz), 15.75 (d, J^3_{CP} = 5.7 Hz). ^{31}P NMR (101 MHz, $CDCl_3$, 25 °C): δ 22.98 ppm. HRMS (ESI) *m/z* calcd for $C_{21}H_{24}NO_3P$ [$M + H^+$]: 392.1401; Found 392.1386.

2.2.5. Diethyl [4-biphenyl (phenylamino) methyl] phosphonate (4e)

White crystalline solid, yield: 86%; mp 158 °C. ^{1}H NMR (300 MHz, $CDCl_3$) δ 7.64–7.53 (m, 6H, HAr), 7.45 (t, *J* = 7.4 Hz, 2H, HAr), 7.36 (t, *J* = 6.7 Hz, 1H, HAr), 7.15 (t, *J* = 7.9 Hz, 2H, HAr), 6.74 (t, *J* = 7.3 Hz, 1H, HAr), 6.66 (d, *J* = 8.1 Hz, 2H, HAr), 4.89 (d, *J* = 7.5 Hz, ^{1}H, HCP), 4.80 (d, *J* = 7.7 Hz, 1H, NH), 4.27–4.09 (m, 2H, –OCH_2–CH_3), 4.01–3.80 (m, 1H, –OCH_2–CH_3), 3.78–3.96 (m, 1H, –OCH_2–CH_3), 1.33 (t, *J* = 7.1 Hz, 3H, –OCH_2–CH_3), 1.18 (t, *J* = 7.1 Hz, 3H, –OCH_2–CH_3). ^{13}C NMR (75 MHz, $CDCl_3$, 25 °C) δ 146.26 (d, *J* = 21.3 Hz), 140.70 (d, *J* = 6.8 Hz), 134.92, 129.22, 128.78, 128.72, 128.23 (d, *J* = 5.4 Hz), 127.35 (d, *J* = 2.9 Hz), 127.29, 127.02, 118.48, 113.88, 63.35 (d, J^2_{CP} = 7.0 Hz), 56.81, 54.82, 16.47 (d, J^3_{CP} = 5.8 Hz), 16.25 (d, J^3_{CP} = 6.1 Hz). ^{31}P NMR (121 MHz, $CDCl_3$, 25 °C): δ 22.58 ppm. HRMS (ESI) *m/z* calcd for $C_{23}H_{26}NO_3P$ [$M + H^+$]: 418.1550; Found 418.1542.

2.2.6. Diethyl [4-methoxyphenyl (phenylamino) methyl] phosphonate (4f)

White crystalline solid, yield: 90%; mp 103 °C. ^{1}H NMR (300 MHz, $CDCl_3$, 25 °C) δ 7.36–7.30 (m, 2H, ArH), 7.07–7.13 (m, 2H, HAr), 6.85 (d, *J*=Hz, 2H, HAr), 6.66 (t, *J* = 16.0 Hz, 1H, HAr), 6.58 (d, 2H, J = Hz, HAr), 4.72 (d, *J* = 24.4 Hz, 1H, CHP), 4.15 (m, 2H, –OCH_2–CH_3), 3.91 (m, 1H, –OCH_2–CH_3), 3.77 (s, 3H, –OCH_3), 3.65–3.74 (m, 1H, –OCH_2–CH_3), 1.28 (t, 3H, *J* = 7.0 Hz, –OCH_2–CH_3), 1.14 (t, 3H, *J* = 7.0 Hz, –OCH_2–CH_3), 4.89 (d, *J* = 7.5 Hz, ^{1}H, HCP), 4.80 (d, *J* = 7.7 Hz, 1H, NH), 4.27–4.09 (m, 2H, –OCH_2–CH_3), 4.01–3.80 (m, 1H, –OCH_2–CH_3), 3.78–3.96 (m, 1H, –OCH_2–CH_3), 1.33 (t, *J* = 7.1 Hz, 3H, –OCH_2–CH_3), 1.18 (t, *J* = 7.1 Hz, 3H, –OCH_2–CH_3). ^{13}C NMR (75 MHz, $CDCl_3$, 25 °C) δ 146.26 (d, *J* = 21.3 Hz), 140.70 (d, *J* = 6.8 Hz), 134.92, 129.22, 128.78, 128.72, 128.23 (d, *J* = 5.4 Hz), 127.35 (d, *J* = 2.9 Hz), 127.29, 127.02, 118.48, 113.88, 63.35 (d, J^2_{CP} = 7.0 Hz), 56.81, 54.82, 16.47 (d, J^3_{CP} = 5.8 Hz), 16.25 (d, J^3_{CP} = 6.1 Hz). ^{31}P NMR (121 MHz, $CDCl_3$, 25 °C): δ 22.58 ppm. HRMS (ESI) *m/z* calcd for $C_{23}H_{26}NO_3P$ [$M + H^+$]: 418.1550; Found 418.1542.

2.2.7. Diethyl [phenyl (p-tolylamino) methyl] phosphonate (4g)

Yield: 94% as a white crystalline solid; mp 120 °C. ^{1}H NMR (300 MHz, $CDCl_3$, 25 °C) δ 7.49–7.47 (m, 2H, HAr), 7.37–7.27 (m, 3H, HAr), 6.93 (d, *J* = 8.3 Hz, 2H, HAr), 6.53 (d, 2H, *J* = 8.4 Hz, HAr), 4.76 (d, *J* = 24.2 Hz, 2H, HCP and NH), 4.17–4.10 (m, 2H, –OCH_2–CH_3), 4.00–3.92 (m, 1H, –OCH_2–CH_3), 3.74–3.66 (m, 1H, –OCH_2–CH_3), 2.20 (s, 3H, CH_3–Ph), 1.30 (t, 3H, *J* = 7.1 Hz, –OCH_2–CH_3), 1.13 (t, 3H, *J* = 7.1 Hz, –OCH_2–CH_3). ^{13}C NMR (75 MHz, $CDCl_3$, 25 °C) δ 143.95 (d, *J* = 15.1 Hz), 135.98, 129.62, 128.50, 127.81 (d, *J* = 4.7 Hz), 127.58, 113.96, 64.83–61.51 (m), 57.54, 55.15, 20.31, 16.27 (dd, J^3_{CP} = 15.2, 5.7 Hz), ^{31}P NMR (101 MHz, $CDCl_3$, 25 °C) δ 21.48 ppm. HRMS (ESI) *m/z* calcd for $C_{18}H_{24}NO_3P$ [$M + H^+$]: 356.1397; Found 356.1386.

2.2.8. Diethyl [4 chlorophenyl (p-tolylamino) methyl] phosphonate (4h)

White crystalline solid, 90% yield, mp 119.5 °C. ^{1} HNMR (300 MHz, $CDCl_3$, 25 °C) δ 7.43 (dd, *J* = 12.0, 4.0 Hz, 2H, HAr), 7.26 (m, 2H, HAr), 6.93(d, 2H, *J* = 8.2 Hz, HAr), 6.48(d, 2H, *J* = 8.5 Hz, HAr), 4.64–4.78(m, 2H, CH–NH), 4.10–4.17(m, 2H, –OCH_2–CH_3), 3.97–4.05(m, 1H, –OCH_2–CH_3), 3.79–3.85(m, 1H, –OCH_2–CH_3), 2.21 (s, 3H, CH_3–Ph), 1.31 (t, 3H, *J* = 7.1 Hz, –OCH_2–CH_3), 1.18 (t, 3H, *J* = 7.1 Hz, –OCH_2–CH_3). ^{13}C NMR (75 MHz, $CDCl_3$, 25 °C) δ 143.85 (d, *J* = 15.0 Hz), 134.84, 133.80, 133.76, 133.71, 129.83, 129.28, 128.21, 127.89, 127.86, 128.03, 114.06, 63.59 (dd, J^2= 12.1, 7.0 Hz), 56.89, 54.89, 20.47, 16.59 (d, J^3_{CP} = 13.7 Hz), 16.52 (d, J^3_{CP} = 5.8 Hz). ^{31}P NMR (121 MHz, $CDCl_3$, 25 °C) δ 22.69 ppm.

2.2.9. Diethyl [4-nitrophenyl (p-tolylamino) methyl] phosphonate (4i)

Yellow crystalline solid, 92% yield; mp 158 °C. ^{1}H NMR (300 MHz, $CDCl_3$, 25 °C) δ 8.21 (d, *J* = 8.5 Hz, 2H, HAr), 7.67 (dd, *J* = 8.8, 2.3 Hz, 2H, HAr), 6.94 (d, 2H, *J* = 8.3 Hz, HAr), 6.46 (d, *J* = 8.4 Hz, 2H, HAr), 4.85 (d, *J* = 25.1 Hz, 2H, HCP + NH), 4.20–4.02 (m, 3H, –OCH_2–CH_3), 3.94–3.86 (m, 1H, –OCH_2–CH_3), 2.35 (s, 3H, CH_3–Ph), 1.32 (t, 3H, *J* = 7.1 Hz, –OCH_2–CH_3), 1.21 (t, 3H, *J* = 7.1 Hz, –OCH_2–CH_3). ^{13}C NMR (75 MHz, $CDCl_3$, 25 °C) δ 147.54, 144.20, 143.25 (d, *J* = 14.8 Hz), 129.86, 128.65 (d, *J* = 4.8 Hz), 128.62, 123.74, 113.93, 63.58 (dd, J^2 CP = 23.8, 6.9 Hz), 57.26, 55.29, 20.36, 16.45 (d, J^3_{CP} = 12.6 Hz), 16.30 (d, J^3_{CP} = 5.8 Hz). ^{31}P NMR (121 MHz, $CDCl_3$, 25 °C) δ 20.94 ppm. HRMS (ESI) *m/z* calcd for $C_{18}H_{24}N_2O_5P$ [$M + H^+$]: 379.1412; Found 379.1417.

2.2.10. Diethyl [4-methoxy phenyl (p-tolylamino) methyl] phosphonate (4j)

White crystalline solid, 90% yield; mp 99 °C. ^{1} HNMR (300 MHz, $CDCl_3$, 25 °C) δ 7.26–7.39 (m, 2H, HAr),6.92(dd, *J* = 16.0, 8.5 Hz, 4H, HAr), 6.49 (d, 2H, *J* = 8.4 Hz, HAr), 4.70 (d, *J* = 24.5 Hz, 2H, CHP–NH),3.99–4.15 (m, 2H, –OCH_2–CH_3),3.91–3.96 (m, 1H, –OCH_2–CH_3), 3.77(s, 3H, –OCH_3), 3.66–3.74 (m, 1H, –OCH_2–CH_3), 2.18 (s, 3H, CH_3Ar), 1.28 (t, 3H, *J* = 7.1 Hz, –OCH_2–CH_3), 1.14 (t, 3H, *J* = 7.1 Hz, –OCH_2–CH_3). ^{13}CNMR (75 MHz, $CDCl_3$, 25 °C) δ159.20, 144.20 (d, *J* = 15.4 Hz), 129.76, 129.08, 129.01, 127.92, 127.88, 127.68, 114.12, 63.38 (dd, J^2 = 6.9, 2.9 Hz), 56.74, 55.34, 54.72, 20.49, 16.63 (d, J^3_{CP} = 14.0 Hz), 16.55 (d, J^3_{CP} = 5.8 Hz). ^{31}P NMR (121 MHz, $CDCl_3$, 25 °C) δ 23.59 ppm.

2.2.11. Diethyl [1-naphtyl (p-tolylamino) methyl] phosphonate (4k)

White crystalline solid, 93% yield; mp 145 °C. ^{1}H NMR (300 MHz, $CDCl_3$, 25 °C) δ 8.27 (d, 1H, J_{HP} = 8.5 Hz, HAr), 7.91 (d, 1H, J = 7.9 Hz, HAr), 7.80–7.77 (m, 2H, HAr), 7.63–7.48 (m, 2H, HAr), 7.45 (t, 1H, J = 7.7 Hz, HAr), 6.67 (d, 2H, J = 8.48 Hz, HAr), 6.48 (d, 2H, J = 8.4 Hz, HAr), 4.64 (d, 1H, J_{HP} = 24.0 Hz, HCP), 4.23–4.15 (m, 2H, –OCH_2–CH_3), 3.77–3.73 (m, 1H, –OCH_2–CH_3), 3.28–3.17 (m, 1H, –OCH_2–CH_3), 2.16 (s, 3H, CH_3–Ph), 1.34 (t, 3H, J = 7.1 Hz, –OCH_2–CH_3), 0.75 (t, 3H, J = 7.1 Hz, –OCH_2–CH_3). ^{13}C NMR (75 MHz, $CDCl_3$) δ 143.83 (d, J = 24.8 Hz), 133.81, 131.6 (d, J = 19.7 Hz), 129.70, 129.00, 128.40, 127.50, 126.22, 125.64, 125.35 (d, J = 6.0 Hz), 123.00, 113.67, 20.33, 16.49 (dd, J^3_{CP} = 5.9, 5.9 Hz). ^{31}P NMR (121 MHz, $CDCl_3$, 25 °C) δ 23.07 ppm. HRMS (ESI) *m/z* calcd for $C_{22}H_{26}NO_3P$ [M + H^+]: 406.1555; Found 406.1542.

2.2.12. Diethyl [4-biphenyl (p-tolylamino) methyl] phosphonate (4l)

White crystalline solid, yield 90%; mp 140 °C. ^{1}H NMR (300 MHz, $CDCl_3$, 25 °C) δ 7.42–7.59 (m, 6H, ArH), 7.26–7.39 (m, 3H, HAr), 6.93 (d, 2H, J = 8.2 Hz, HAr), 6.55 (d, 2H, J = 8.4 Hz, HAr), 4.79 (d, 1H, J = 24.3 Hz, HCP), 4.10–4.18 (m, 2H, –OCH_2–CH_3), 3.84–4.01 (m, 1H, –OCH_2–CH_3), 3.71–3.81 (m, 1H, –OCH_2–CH_3), 2.19 (s, 3H, CH_3Ar), 1.30 (t, 3H, J = 7.1 Hz, –OCH_2–CH_3), 1.15 (t, 3H, J = 7.0 Hz, –OCH_2–CH_3). ^{13}C NMR (75 MHz, $CDCl_3$, 25 °C) δ 143.82, 140.59, 129.67, 128.70, 128.20 (d, J = 5.5 Hz), 127.66, 127.24 (d, J = 2.7 Hz), 126.96, 113.98, 63.31 (t, J = 7.0 Hz), 57.28, 54.87, 20.33, 16.38 (d, J^3_{CP} = 14.0 Hz), 16.16 (d, J^3_{CP} = 5.5 Hz) ^{31}P NMR (121 MHz, $CDCl_3$, 25 °C): δ 22.71 ppm. HRMS (ESI) *m/z* calcd for $C_{24}H_{29}NO_3P$ [M + H^+]: 410.1876; Found 410.1879.

2.2.13. Diethyl [4-nitro phenyl (p-tolylamino) methyl] phosphonate (4m)

White crystalline solid, yield 80%; mp 137 °C. ^{1}H NMR (360 MHz, Chloroform-*d*) δ 8.08–8.00 (m, 2H, HAr), 7.36 (dd, J = 8.2, 2.2 Hz, 3H, HAr,), 7.19 (d, J = 8.2 Hz, 2H, HAr), 6.65–6.57 (m, 2H, HAr), 4.80 (dd, J = 23.7, 7.6 Hz, 1H, *CH), 4.25–4.07 (m, 2H, –OCH_2–CH_3), 3.96 (m, 1H, –OCH_2–CH_3), 3.76–3.59 (m, 1H, –OCH_2–CH_3), 2.36 (d, J = 1.9 Hz, 3H, CH_3Ar), 1.34 (t, J = 7.0 Hz, 3H, –OCH_2–CH_3), 1.16 (t, J = 7.3 Hz, 3H, –OCH_2–CH_3). ^{13}C NMR (91 MHz, Chloroform-*d*) δ 138.36 (d, J = 3.6 Hz), 131.40 (d, J = 3.3 Hz), 129.90–129.35 (m), 127.61 (d, J = 5.4 Hz), 126.05, 112.45, 63.54 (dd, J = 48.3, 7.1 Hz), 56.18, 54.50, 16.43 (d, J^3_{CP} =5.8 Hz), 16.20 (d, J^3_{CP} = 5.7 Hz). ^{31}P NMR (101 MHz, Acetone-d_6) δ 21.39. HRMS (ESI) *m/z* calcd for $C_{18}H_{23}N_2NaO_5P$ [M + Na^+]: 401.1239; Found. 401.1222.

2.2.14. Diethyl [2-methoxyphenyl (4-bromo,2,6-dimethylamino) methyl] phosphonate (4n)

White crystalline solid, yield 92%; mp 106.8 °C. ^{1}H NMR (360 MHz, Chloroform-*d*) δ 7.65 (d, J = 11.1 Hz, 2H, ArH), 7.27 (d, J = 9.9 Hz, 1H, ArH), 7.04 (d, J = 18.1 Hz, 3H, ArH), 6.85 (d, J = 8.3 Hz, 1H, ArH), 5.25 − 5.02 (m, 1H, –OCH_2–CH_3), 4.33 − 4.06 (m, 2H, –OCH_2–CH_3), 3.96 − 3.84 (m, 1H, –OCH_2–CH_3), 3.75 (s, 3H, –OCH_3), 3.71 − 3.58 (m, 1H, –OCH_2–CH_3), 2.24 (s, 6H, 2CH_3Ar), 1.29 (t, J = 7.1 Hz, 3H, –OCH_2–CH_3), 1.05 (t, J = 7.1 Hz, 3H, –OCH_2–CH_3). ^{13}C NMR (91 MHz, Chloroform-*d*) δ 156.79 (d, J = 7.3 Hz), 143.86 (d, J = 9.1 Hz), 131.08 (d, J = 5.3 Hz), 129.06, 125.86, 120.90 (d, J = 1.9 Hz), 113.70, 110.74, 63.23 − 62.23 (m), 55.62, 16.23 (dd, J^3_{CP} = 22.3, 5.7 Hz). ^{31}P NMR (101 MHz, Acetone-d_6 25 °C) δ 24.89 ppm. HRMS (ESI) *m/z* calcd for $C_{20}H_{28}BrNNaO_4P$ [M + Na^+]: 478.0753; Found 478.0742.

2.2.15. Diethyl [3-methoxyphenyl (4-bromo,2,6-dimethylamino) methyl] phosphonate (4o)

White crystalline solid, yield 88%; mp 113 °C. ^{1}H NMR (360 MHz, Chloroform-*d*) δ 7.33–7.21 (m, 1H, ArH), 7.07 (s, 2H, ArH), 7.06–6.95 (m, 2H, ArH), 6.85 (d, J = 9.2 Hz, 1H, ArH), 4.53 − 4.34 (m, 1H, *CH), 4.23 − 4.09 (m, 2H, –OCH_2–CH_3), 3.95 (m, 1H, –OCH_2–CH_3), 3.81 (s, 3H, –OCH_3), 3.74–3.59 (m, 1H, –OCH_2–CH_3), 2.23 (s, 6H, 2CH_3Ar), 1.31 (t, J = 7.1 Hz, 3H, –OCH_2–CH_3), 1.09 (t, J = 7.1 Hz, 3H, –OCH_2–CH_3). ^{13}C NMR (91 MHz, Chloroform-*d*) δ 131.35, 130.90, 129.42, 120.61 (d, J = 6.4 Hz), 113.80 (dd, J = 22.6, 15.9 Hz), 62.93 (dd, J = 34.7, 7.2 Hz), 18.73, 16.39 (d, J^3_{CP} = 6.2 Hz), 16.14 (d, J^3_{CP} = 5.9 Hz). ^{31}P NMR (101 MHz, Acetone-d_6, 25 °C) δ 23.93 ppm. HRMS (ESI) *m/z* calcd for $C_{20}H_{27}BrNNaO_4P$ [M +Na^+]: 478.0753; Found 478.0738.

2.2.16. Diethyl [4-trifluoromethyl phenyl (phenylamino) methyl] phosphonate (4p)

White crystalline solid, yield 80%; mp 140 °C. ^{1}HNMR (300 MHz, $CDCl_3$, 25 °C) δ 1.12 (t, 3H, J = 7.0 Hz, –OCH_2–CH_3), 1.31 (t, 3H, J = 7.1 Hz, –OCH_2–CH_3), 3.61–3.70 (m, 1H, –OCH_2–CH_3), 3.90–4.08 (dp, J = 10.1, 7.1 Hz, 1H, –OCH_2–CH_3), 4.10–4.20 (m, 2H, –OCH_2–CH_3), 4.79 (dd, 1H, J = 24.2, 7.5 Hz, Ph–CH), 5.16–5.31 (m, 1H, NH), 6.62 (d, 2H, J = 8.5 Hz, HAr), 7.26–7.40 (m, 5H, HAr),7.49 (dd, J = 7.7,2.1 Hz, 2H, HAr).^{13}CNMR (75 MHz, $CDCl_3$, 25 °C) δ 148.90 (d, J = 14.4 Hz), 135.13(d, J = 3.0 Hz), 128.91, 128.87, 128.38, 128.34, 127.90, 127.83, 126.68, 126.63, 113.16, 63.75 (dd, J^2_{CP} = 22.9,7.0 Hz), 56.77, 54.77, 16.59 (d, J^3_{CP} = 19.0 Hz), 16.51 (d, J^3_{Cp} = 5.8 Hz).^{31}P NMR (121 MHz, $CDCl_3$, 25 °C) δ = 22.54 ppm.

2.2.17. Diethyl [4-chlorophenyl (4-trifluoromethylphenylamino) methyl] phosphonate (4q)

White crystalline solid, yield 80%; mp 129 °C. ^{1}HNMR (300 MHz, $CDCl_3$, 25 °C): δ = 1.18 (t, 3H, J = 6.9 Hz, –OCH_2–CH_3), 1.32 (t, 3H, J = 7.1 Hz, –OCH_2–CH_3), 3.72–3.81 (m, 1H, –OCH_2–CH_3), 3.96–4.01(m,1H, –OCH_2–CH_3),4.04–4.18 (m, 2H, –OCH_2–CH_3), 4.70 (dd, 1H, J = 24.4,7.3 Hz,CHP),5.16 (dd, 1H, J = 10.2, 7.5 Hz, –NH), 6.60 (d, 2H, J = 8.6 Hz, HAr), 77.28–7.43 (m, 6H, HAr).^{13}CNMR (75 MHz, $CDCl_3$, 25 °C) δ 148.61 (d, J = 14.2 Hz),134.24 (d, J = 3.9 Hz), 134.19, 133.96, 133.92, 129.19, 129.12, 126.76, 126.71, 113.19, 63.71 (dd, J^2 = 11.2, 7.0 Hz), 56.27, 54.27, 16.60 (d, J^3_{CP} = 13.9 Hz),16.53 (d, J^3_{CP} = 5.7 Hz). ^{31}P NMR (121 MHz, $CDCl_3$, 25 °C) δ 21.87 ppm.

2.2.18. Diethyl [4-methoxyphenyl (4-trifluoromethylphenylamino) methyl] phosphonate (4r)

White crystalline solid, yield 88%; mp 111 °C. ^{1}HNMR (300 MHz, $CDCl_3$, 25 °C) δ 7.26–7.40 (m, 4H, HAr), 6.90 (d, 2H, *J* = 8.5 Hz, HAr), 6.63 (d, 2H, *J* = 8.5 Hz, HAr), 5.15 (dd, *J* = 9.7,7.8 Hz, 1H, –NH), 4.73 (dd, 1H, *J* = 23.8, 7.6 Hz, CHP), 4.13 (m, 2H, $–OCH_2–CH_3$), 3.95 (m, 1H, $–OCH_2–CH_3$), 3.80 (s, 3H, $–OCH_3$), 3.63–3.72 (m, 1H, $–OCH_2–CH_3$), 1.31 (t, 3H, *J* = 7.1 Hz, $–OCH_2–CH_3$), δ 1.15 (t, 3H, *J* = 7.0 Hz, $–OCH_2–CH_3$). ^{13}C NMR (75 MHz, $CDCl_3$, 25 °C) δ 159.60, 148.16 (d, *J* = 14.3 Hz), 128.97, 126.96, 126.67, 114.35 (d, *J* = 2.3 Hz), 113.19, 63.70 (dd, J^2=24.1,7.0 Hz), 56.10, 55.38, 54.08, 16.61 (d, J^3_{CP} = 13.9 Hz), 16.54 (d, J^3_{CP} = 5.8 Hz). ^{31}P NMR (121 MHz, $CDCl_3$, 25 °C) δ 22.77 ppm.

2.3. Computational details

2.3.1. Quantum chemical calculations

All quantum chemical calculations were performed using DFT method in the Gaussian 09 program package (Frisch et al., 2009). Gauss View 5.0.8 computer program was used to visualize the results (Dennington et al., 2009). The geometries were optimized at the long-range corrected (CAM-B3LYP) functional (Yanai et al., 2004) with standard 6-31G (d, p) basis set (Becke, 1993). The calculated energies of the highest occupied molecular orbital (E_{HOMO}) and lowest unoccupied molecular orbital (E_{LUMO}) have been used to determine various quantum chemical parameters such as the energy gap (ΔE_{gap}), the dipole moment (μ), chemical hardness (η), chemical softness (σ), electronegativity (χ) and global electrophilicity index (ω), using the following equations (Feng et al., 2018; Kohn & Sham, 1965; Rogova et al., 2021). AQ3

$$\Delta E_{gap} = E_{LUMO} - E_{HOMO} \quad (1)$$

$$\eta = \frac{E_{LUMO} - E_{HOMO}}{2} \quad (2)$$

$$\sigma = \frac{1}{\eta} \quad (3)$$

$$\chi = -\frac{(E_{HOMO} + E_{LUMO})}{2} \quad (4)$$

$$\omega = \left(\frac{\chi^2}{2\eta}\right) \quad (5)$$

2.3.2. In silico drug-likeness and ADMET prediction

In order to screen the physicochemical characteristics, pharmacokinetic behavior and the drug likeness; in *silico* ADME (Absorption, Distribution, Metabolism and Excretion) parameters and toxicity prediction of the designed compounds were calculated using the SwissADME (http://www.swissadme.ch) (Daina et al., 2017). Lipinski's rule of five, Ghose, Veber, Egan, Muegge and synthetic accessibility were prerequisite to ensure drug-like properties when using rational drug design. (mol. wt. ≤ 500 Da; log P o/*w* ≤ 5; HBD ≤ 5; HBA ≤ 10). Solubility (LogS): Should be > −4. Van der Walls topological polar surface area (TPSA) value is (≤140 $Å^2$) (Lipinski, 2016; Olasupo et al., 2020).

2.3.3. Molecular docking studies

A molecular docking study of the three α-aminophosphonates synthesized (**4p, 4q** and **4r**) and Adriamycin (ADM) taken as reference was performed using Auto-DockTools (ADT) (Morris et al., 2009), software and AutoDock Vina program, (Oleg & Olson, 2010), and the 3D structure of target protein Human topoisomerase IIα (PDB ID: 1ZXM, Resolution: 1.87 Å) (Wei et al., 2005) was obtained from RCSB protein data bank. All ligands were geometrically optimized by DFT calculation. The docked poses and ligand-protein interactions were visualized using the Discover Studio Visualizer software (Chung-Kiak & Han-Ping, 2016). The analysis of the docked models was performed to investigate the binding affinity and the nature of the intermolecular bonding interactions between each species and the target proteins. The modes of interactions of the ligand with proteins were determined by investigating their favorable orientations of binding.

3. Results and discussion

3.1. Synthesis

Herein, in our quest for developing the optimization reaction conditions we performed using the condensation of aromatic aldehyde (1 mmol), aniline (1 mmol) and diethylphosphite (1.2 mmol) as study model. First, we have used blank reaction without catalyst then we have investigated the effect of several crown ethers as organocatalysts in the multicomponents reaction for the synthesis of α-aminophsphonate. To determine the best catalyst, we have selected: 18-crown-6 **(A)**, 15-crown-5 **(B)**, 12-crown-4 **(C)**, 2-hydroxymethyl-18-crown-6 **(D)** and bibenzo-18-crown-6 **(E)** (Figure. 1). All these catalysts were loading at 5 mol%, and the reactions carried in THF at room temperature within 24 h.

Figure 1. Crown ethers tested.

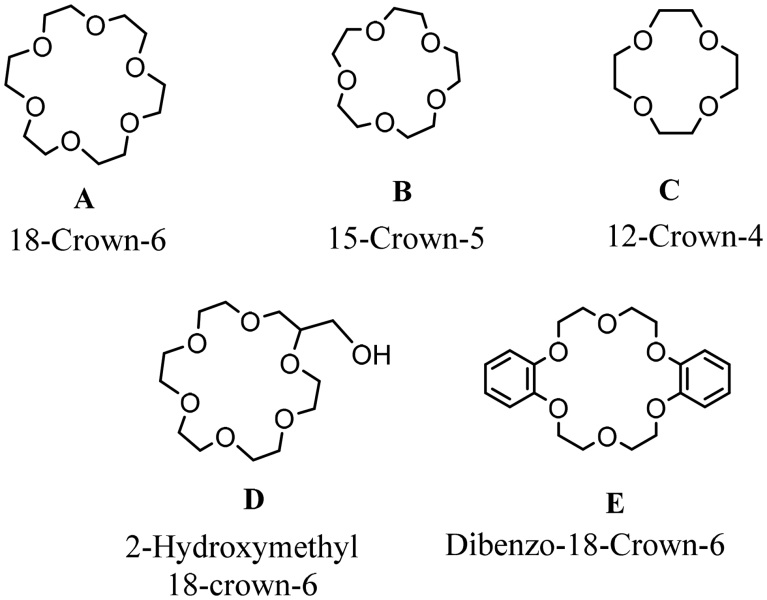

The obtained results show that no reaction was observed without catalyst (Table 1, entry 1), and traces of products appear using the organocatalysts chosen whatever the crown's size, such as; 18-crown-6 **(A),** 15-crown-5 **(B)**, 12-crown-4 **(C)** and dibenzo-18-crown-6 (**E)** (Table 1, entries 2, 3, 4 and 6). Therefore, the hydroxymethyl linked to 18-crown-6 **(D**) led to obtain the desired product with excellent yield (91%) (Table 1, entry 5). These results explained by the efficiency of the catalyst to activate the carbonyl of aromatic aldehyde which facilitate the nucleophilic attack of diethylphosphite. The best recorded results were shown using of 2-hydroxymethyl-18-crown-6 **(D)** (5 mol %) in THF (2 mL) at room temperature giving the α-aminophosphonate **4a** in 91% yield.

Note: The table layout displayed in 'Edit' view is not how it will appear in the printed/pdf version. This html display is to enable content corrections to the table. To preview the printed/pdf presentation of the table, please view the 'PDF' tab.

Table 1. Different catalysts tested.[a]

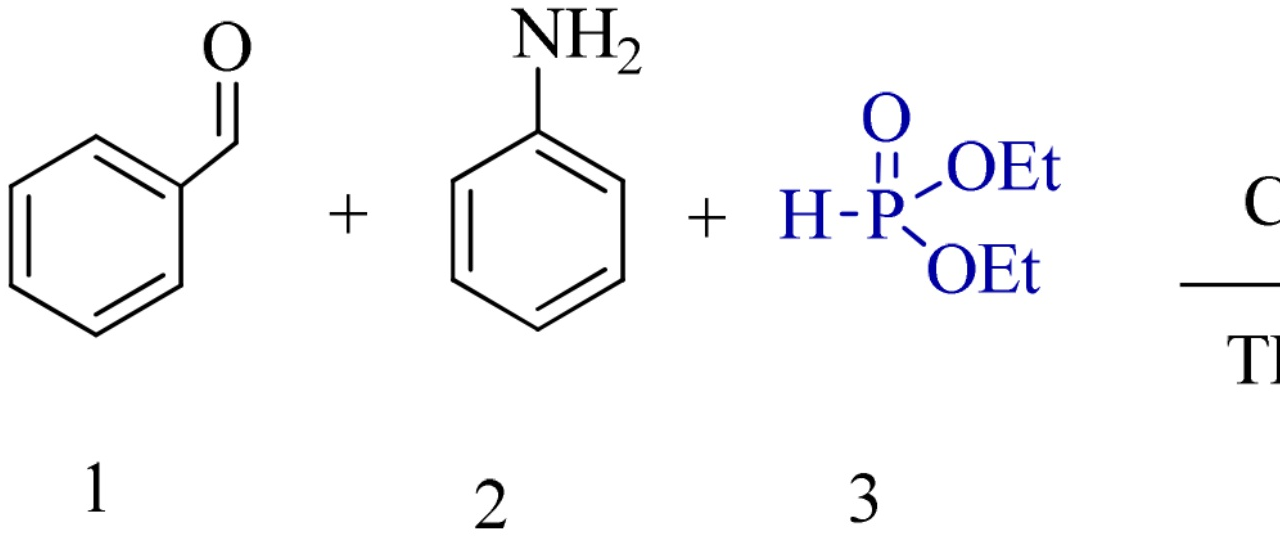

Entry	Catalyst (5 mol%)	Yield (%)[c]
1[b]	Free-catalyst	–
2	18-Crown-6 **(A)**	Traces
3	15-Crown-5 **(B)**	Traces
4	12-Crown-4 **(C)**	Traces
5	**2-Hydroxymethyl-18-crown-6 (D)**	**91**
6	Dibenzo-18-crown-6 **(E)**	Traces

[a]Reaction conditions: benzaldehyde (1 mmol), aniline (1 mmol) and diethylphosphite (1.2 mmol) were stirred with catalyst (5 mol%) in THF (2 mL) at room temperature, within 24 h.

[b]Reaction without catalyst.

[c]Yield of the pure product purified by crystallization in hexane.

Owing the encouraged results obtained with the 2- hydroxymethyl-18-crown-6 **(D)** described above, we have envisaged to checking the impact of the hydrophobicity-hydrophilicity of the organic medium on the outcome of our optimized reaction. For that, several organic solvents have been tested, such as: THF (logP = 0.46), EtOH (logP = −0.18), CH_2Cl_2 (logP = 1.25), CH_3CN (logP = −0.37), AcOEt (logP = 0.73) and TBME (logP = 0.35). The recorded results reveal that no significant correlation between the chemical yields of the product **4a** and the logP coefficient. The best result was recorded in THF as solvent giving the desired product with excellent yield (91%). Low yields of the reactions were observed in TBME, AcOEt and CH_2Cl_2 (<30%), while 40% chemical yield was obtained in CH_3CN. In EtOH, the desired product was recovered in 66% yield under the same conditions, which illustrated in Figure. 2. The α-aminophosphonate was easily obtained by crystallization from hexane. In addition, it is important to underline the total disappearance of all reagents in THF within 15 min of stirring.

Figure 2. Impact of the organic solvent hydrophobicity's (reaction conditions: 2-hydroxymethyl-18-crown-6 (5 mol%), 2 mL of solvent, rt, 24 h).

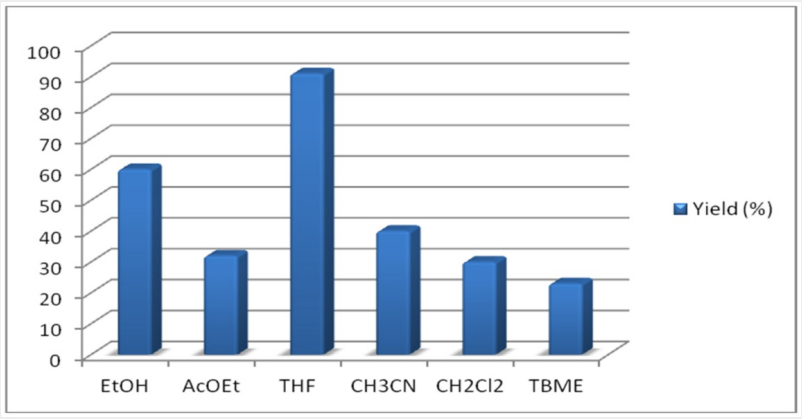

In order to validate the optimum conditions using 2-Hydroxymethyl-18-crown-6 **(D)**, we applied them on a set of substituted benzaldehyde and aniline with electron-withdrawing and electron-donating. The results summarized in Table 2 showed the efficiency of 2-hydroxymethyl-18 crown-6 **(D)**, used as novel organocatalyst in the MCRs by *Kabachnik–Fields* reaction for P-C bond formation by α-aminophosphonates preparation.

Note: The table layout displayed in 'Edit' view is not how it will appear in the printed/pdf version. This html display is to enable content corrections to the table. To preview the printed/pdf presentation of the table, please view the 'PDF' tab.

Table 2. 2-Hydroxymethyl-18-crown-6 catalyzed the synthesis of diethyl α-aminophosphonates 4a–r.[a]

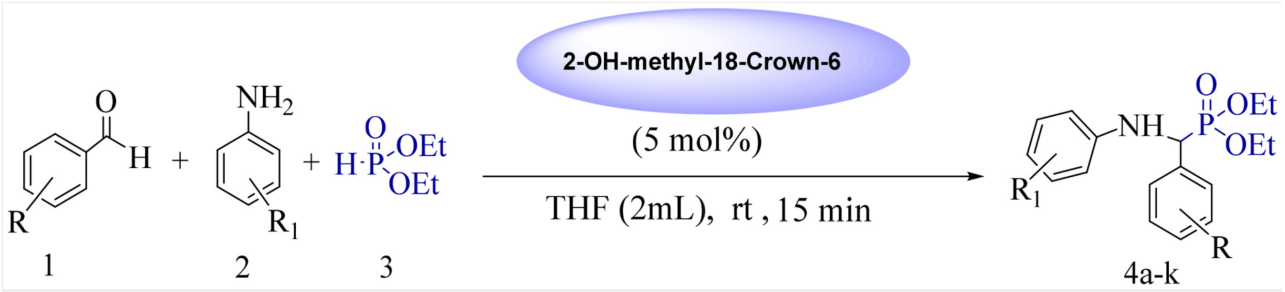

Product **4a–r** (yield)[b]		
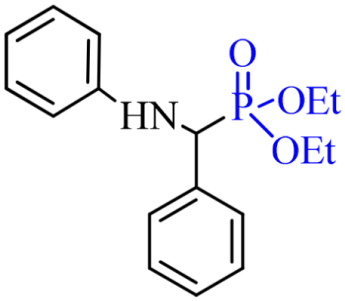 4a (91%)	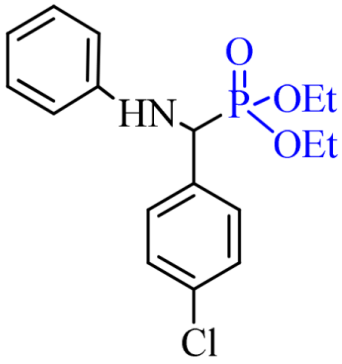 4b (80%)	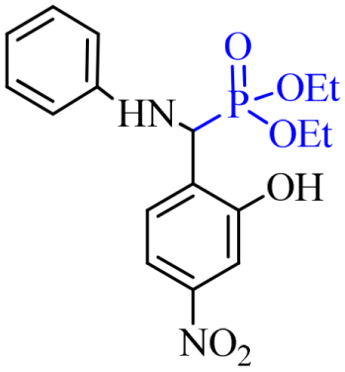 4c (93%)
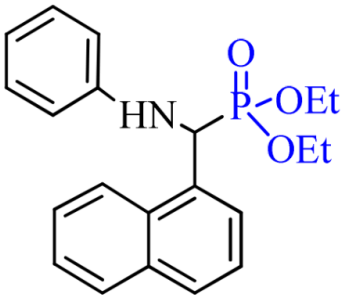 4d(88%)	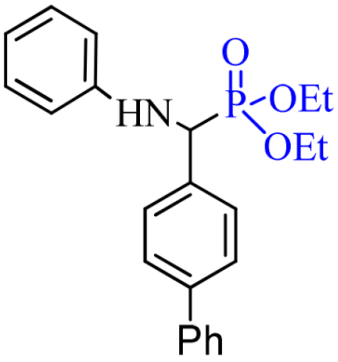 4e (86%)	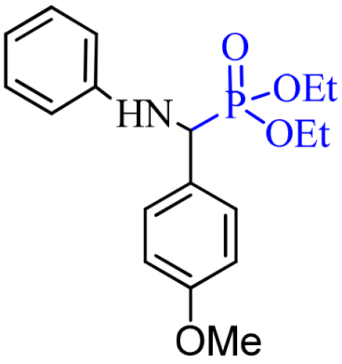 4f (90%)

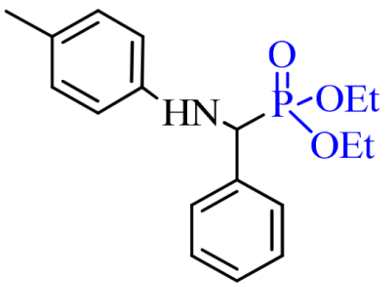

4g (94%)

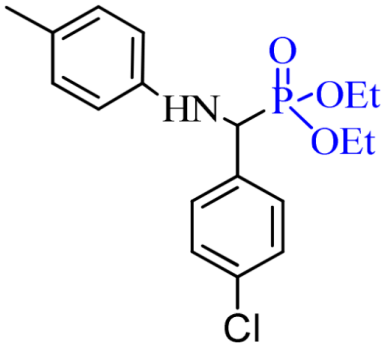

4h (90%)

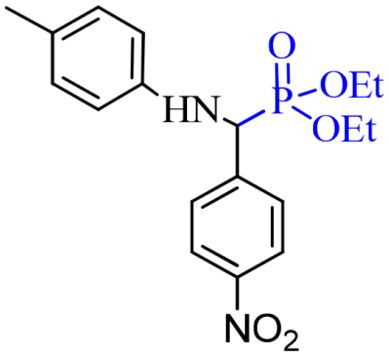

4i (92%)

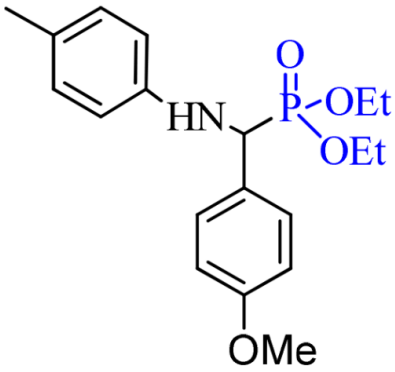

4j (90%)

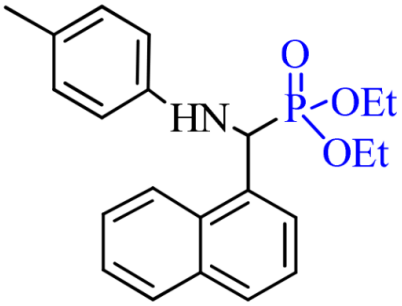

4k (93%)

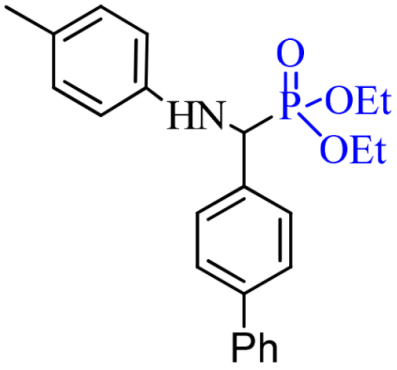

4l (90%)

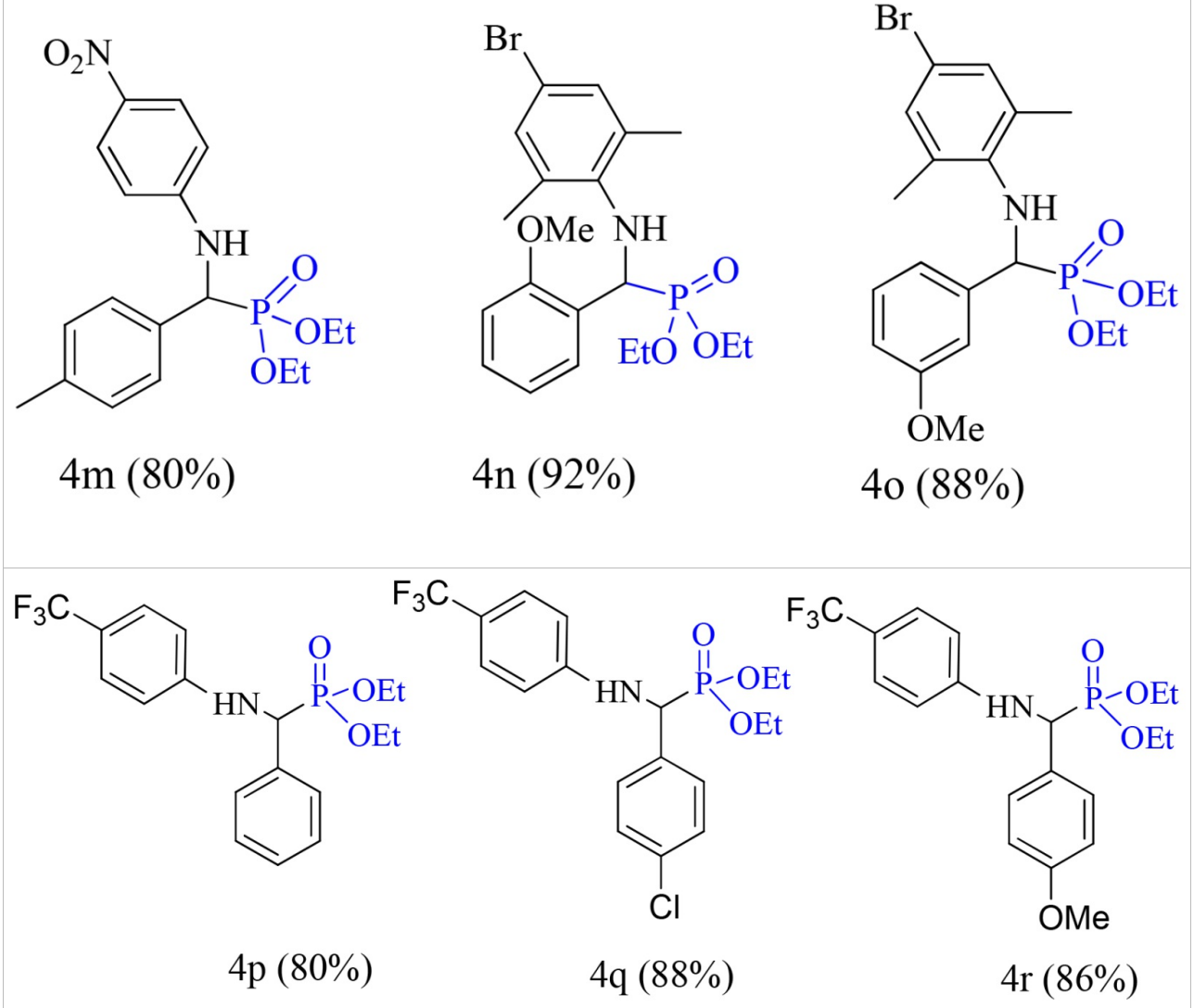

[a]Reaction conditions: aromatic aldehyde (1 mmol), aniline (1 mmol), diethylphosphite (1,2 mmol), 2-hydroxymethyl-18-crown-6 (5 mol%), room temperature, in THF within 15 min.

[b]Isolated yield after purification by crystallization from hexane.

All the chemical yields showed in the Table 2 were obtained by crystallization in hexane. The chemical yields of multicomponent reactions depend on the nature of electronic effects of the substrates. The use of benzaldehyde, 4-chlorobenzaldehyde, 4-nitrobenzaldehyde, 1-naphtaldehyde, 4-phenylbenzaldehyde and 4-methoxybenzaldehyde with aniline leads, respectively to **4a**, **4b, 4c 4d, 4e** and **4f** with yields between 80 and 93%. Similarly, using toluidine with the above series of aromatic aldehydes gives the **4g**, **4h, 4i, 4j, 4k** AQ4 and **4l** with best results up to 90% yields, this due to the electron donating of toluidine.

The use of 4-nitroaniline with tolylbenzaldehyde gives the desired product **4m** with 80%, and the two products **4n** and **4o** are obtained with 92 and 88% yields by using 4-bromo, 2,6-dimethylaniline with 2-methoxy and 3 methoxy benzaldehyde respectively. The employ of 4-trifluoromethananiline with benzaldehyde, 4-chlorobenzaldehyde and 4-methoxybenz-aldehyde gives the α-aminophosphonaes **4p, 4q** and **4r** with 80%, 88% and 86% chemical yields respectively.

In order to understand the mechanism for the synthesis of α-aminophosphonates by multicomponents reaction using 2-hydroxymethyl-18-crown-6 as catalyst, we tested some other alcohols as catalysts in the same conditions, such as: ethanol, phenol and 2-hydroxymethyl phenol. The results show that traces of desired product were obtained using ethanol and phenol, however, a good yield (60%) was obtained using 2-hydroxymethyl phenol. In our case, we confirmed that the efficiency of 2-hydroxymethyl-18 crown-6 is due to the hydrogen bond with OH and the specificity of the crown ether cavity. Combining the viewpoints developed by our previous work (Aissa et al., 2022; Lakoud et al., 2016), and based on our above described observations, we proposed herein a mechanism for the multicomponents reaction using 2-Hydroxymethyl-18 Crown-6 as catalyst, as summarized in Scheme 1. However, we suppose that this organocatalyst plays a crucial role for the P–C bond formation. First, the 2-hydroxymethyl-18 Crown ether-6 probably coordinates the oxygen of benzaldehyde to accelerate the nucleophilic attack of aniline to form an imine, then the 2-hydroxymethyl-18 crown ether-6 coordinates the imine by hydrogen bond to facilitate the nucleophilic attack of diethylphosphite to obtain the desired product.

Scheme 1. Proposed mechanism of 2-hydroxymethyl-18-crown ether-6 catalyzed α-aminophosphonates synthesis.

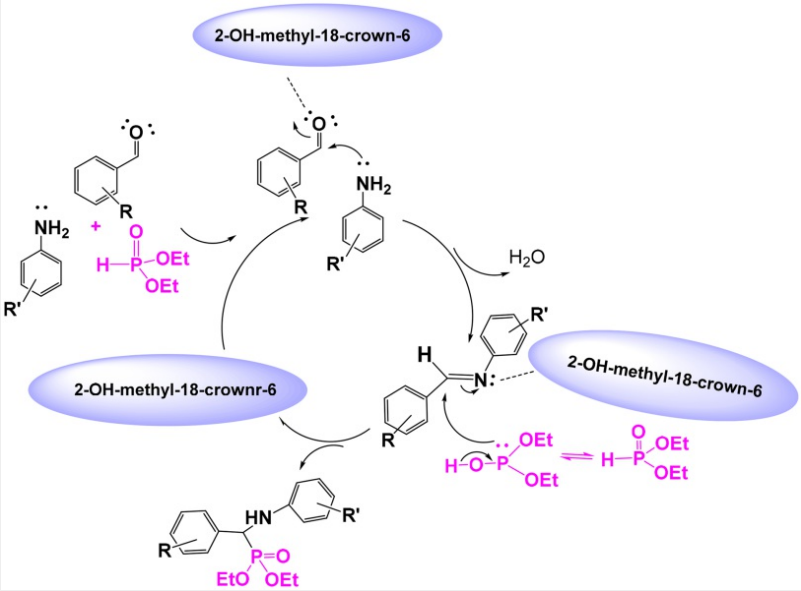

Due to wide medicinal applications of fluorinated α-aminophosphonates compounds, many studies have reported the interesting biological properties of trifluoromethyl α-aminophosphonates derivatives, which showed the cytotoxic activity toward cancer cells (Kandula et al., 2017; Satish et al., 2018). Herein, we have scrutinized the three synthesized α-aminophosphonates (**4p, 4q** and **4r**) in quantum chemical calculations and modeling molecular study to determine the minimum energy molecular structure and to understand the correlation between the biological activity of α-aminophosphonates and their molecular structures (Cytlak et al., 2017; Turcheniuk et al., 2013).

3.2. DFT study

3.2.1. Optimization of structures

The geometry optimization of molecules synthesized (**4p**, **4q** and **4r**) was performed by minimizing the energy using DFT method at the CAM-B3LYP level with the base 6-31 G (d, p), and showed in Figure 3. The calculated values of total energy for each molecule at the optimal stage were: −1619.4040 a.u, −2078.9989 a.u and −1733.8816 a.u respectively, which signify the energy of the more stable conformation of the studied structures.

Figure 3. Theoretical optimized structures of **4p, 4q** and **4r** with CAM-B3LYP/6-31G (d,p) method.

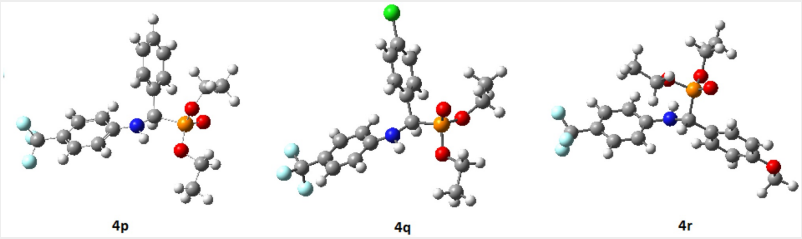

3.2.2. Frontier molecular orbital analysis

Frontier Molecular Orbitals HOMO (Highest Occupied Molecular Orbital) and LUMO (Lowest Unoccupied Molecular Orbital), or HOMO is directly related to ionization

potential and can examined the aptitude of a molecule to contribute electrons to an electrophilic species, and LUMO is directly related to electron affinity and can determine the ability of a molecule to accept electrons from nucleophilic species (Elfily, 2020; Xavier & Periandy, 2015). These orbitals can describe significantly the stability and reactivity of drug molecules (Abraham et al., 2017; Asiri et al., 2011). So, the capacity of a molecule to give electrons to an acceptor species is favored by the high values of E_{HOMO}, whereas the ability of a molecule to take electrons is preferred by the low values of E_{LUMO} (Mekky et al., 2015). Furthermore, the estimated value of HOMO-LUMO energy (ΔEgap) of drug molecules shows the energy required to excite a molecule's electrons. If the ΔE_{gap} is small, molecules can be highly chemically reactive and unstable and readily excited, whereas if the ΔE_{gap} is big, molecules can be very stable and less chemically reactive (Kosar & Albayrak, 2011).

Higher value of E_{HOMO} indicates a better tendency toward the donating electrons, the Table 3 show that the molecule **4p** and **4q** (E_{HOMO} = −7.202 eV and −7.309 eV) respectively are the most molecules have the ability to accept electrons, while **4r** has the highest HOMO energy (E_{HOMO} = −7.1021 eV) that allows it to be the best electron donor molecule.

Note: The table layout displayed in 'Edit' view is not how it will appear in the printed/pdf version. This html display is to enable content corrections to the table. To preview the printed/pdf presentation of the table, please view the 'PDF' tab.

Table 3. Calculated quantum chemical parameters of 4p, 4q and 4r using DFT/CAM-B3LYP/6-31G (d,p) method.

Compounds	E_{HOMO} (ev)	E_{LUMO} (ev)	ΔE (ev)	Dipole moment DM(D)	Hardness η (ev)	Softness σ (ev)	Electronegativity χ (ev)	Electrophilicity ω (ev)
4p	–7.202	0.8846	8.0866	5.0913	4.0433	0.2473	3.1587	1.2338
4q	–7.3097	0.6049	7.9146	6.0432	3.9573	0.2526	3.3524	1.4199
4r	–7.1021	0.9088	8.0109	3.2374	4.0054	0.2496	3.0966	1.1969

Place the cursor position on table column and click 'Add New' to add table footnote.

The calculations show that the energy gap of **4p**, **4q** and **4r** are 8.0866 eV, 7.9146 eV and 8.0109 eV respectively as shown in Table 3, the compounds **4p** and **4r** have relatively higher energy gap than **4q,** which signifies the liberation of electrons to an acceptor molecule. Moreover, the calculated value of Δ Egap indicates the highly reactive molecules.

Figure 4 illustrates the calculated HOMO and LUMO orbitals for the **4p, 4q** and **4r** ligands of α-aminophosphonates derivatives, which revealed that the HOMO and LUMO are frequently located on the aromatic ring and the amino group and on CF_3 group just for HOMO. On the outer hand, Table 3 shows that the studied molecules have an elevated value of E_{LUMO} and lower of E_{HOMO}.

Figure 4. HOMO and LUMO orbitals of **4p, 4q** and **4r** with CAM-B3LYP/6-31G (d,p) method.

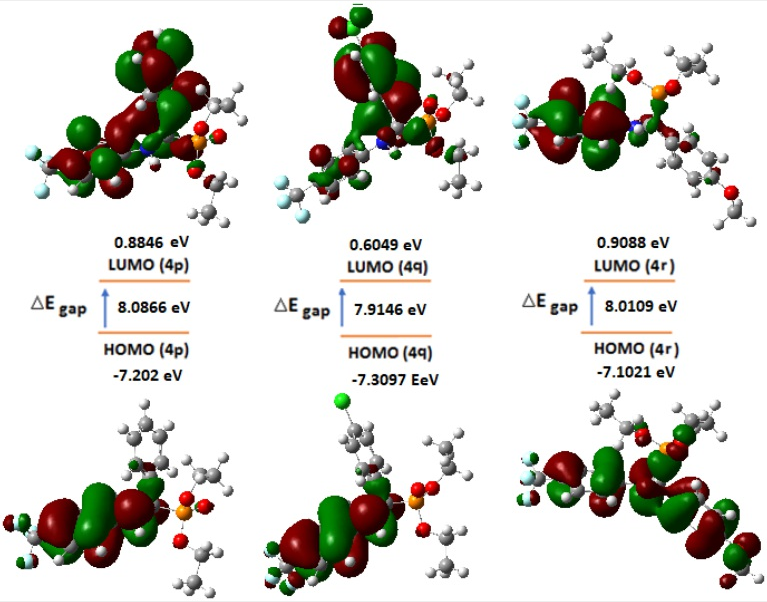

3.2.3. Global reactivity descriptors

The polarity of pharmacological molecules is denoted by the dipole moment (μ), which is an important electronic property that results from the non-uniform distribution of charges on the different atoms. Table 3 shows that the calculated values of dipole moments in the case of **4q** (6.0432 D) is more superior than **4p** and **4r** (5.091 D and 3.2374 D) respectively, it can be explained by the difference in electronegativity caused by Cl. Furthermore, the hardness (η) and local softness (σ) of drug molecules can be used to assess their resistance to deformation of their electron clouds or polarization (Raafat et al., 2008). These two descriptors are essential properties to measure reactivity and the molecular stability of molecules. Chemical hardness corresponds to the energy gap between the LUMO and HOMO. The larger energy gap indicates that the molecule is harder and more stable therefore less reactive. As shown in Table 3, it can be seen that the three compounds **4p, 4q** and **4r** are stable because they present high values of hardness (4.033, 3.9573 and 4.0054 eV).

Electronegativity (χ) is the tendency to attract electrons of an atom, molecule or solid substance to itself. The calculated electronegativity of **4p, 4q** and **4r** is found to be 3.1587, 3.3524 and 3.0966 eV respectively. The electrophilicity index (ω) measures the capacity of species to accept electrons (the electrophilic tendency). We can divide organic molecules into three categories based on their electrophilicity values: marginal electrophiles with a value of less than 0.8 eV, moderate electrophiles between 0.8 and 1.5 eV, and strong electrophiles with a value greater than 1.5 eV (Domingo et al., 2002). In this case, all values of 1.2338 eV, 1.4199 eV and 1.1969 eV for the investigated ligands **4p, 4q** and **4r** respectively are moderate electrophiles.

3.2.4. Molecular electrostatic potential

The molecular electrostatic potential (MEP) is an important parameter to be predicted to verify the evidence regarding the investigated reactivity of the compounds as enzyme inhibitors, it can be an indicator for expecting physiochemical property relationships with the molecular structure to determine the efficient centers accountable for electrophilic and nucleophilic reactions. Moreover, MEP is associated to the electronic density. The negative regions of MEP are related to electrophilic reactivity demonstrated in the red color, and the positive ones to nucleophilic reactivity demonstrated in blue color.

The visualization of the Figure 5 show that negative potentials are presented at electronegative oxygen atoms attached to the phosphorous group O21 and O26, whereas positive potentials are presented at hydrogen atoms for all compounds. Obviously through Figure 5 that for the considered inhibitors, the possible sites for electrophilic attack are generally located at heteroatom. Otherwise, the phenyl rings of the considered compounds have a negative region. It is clear from the obtained zones of MEP that the negative possible positions are about electronegative atoms (N and O) and the conjugated double bonds, contrariwise the positive possible zones are about the hydrogen atoms.

Figure 5. Molecular electrostatic potentials (MEP) for the investigated compounds.

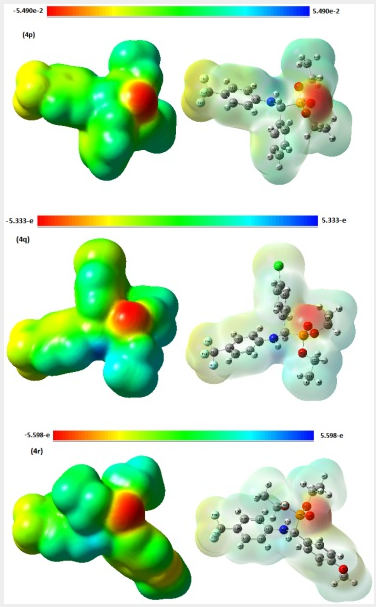

3.3. Molecular docking studies

In *silico* molecular docking was applied to probe interactions of ligand with protein. Prior to the docking calculations, water molecules around the enzyme were removed, hydrogen atoms were added and the *Kollman* charge was calculated. The active site of 1ZXM was done by re-docking with ANP (phosphoaminophosphonic acid adenylate ester) onto the binding site (Asn 163, Tyr 165, Glu 87, Thr 147, Ile 125, Asn 91, Asn 120, Ser 148, Ser 149, Phe 142, Thr 215, Asn 95, Gln 376, Arg 162, Lys 168) (Figure 6) (Wei et al., 2005). The binding site parameters obtained are ($X = 36.548$, $Y = -1.089$; $Z = 34.656$ and size $x = 40$, $y = 40$, $z = 40$). The RMSD index of binding topology between the original ligand and re-docked ligand onto the active site is 1.9438 Å.

Figure 6. Crystalline structure of Human topoisomerase IIα (PDB ID: 1ZXM). A: No prepared, B: prepared.

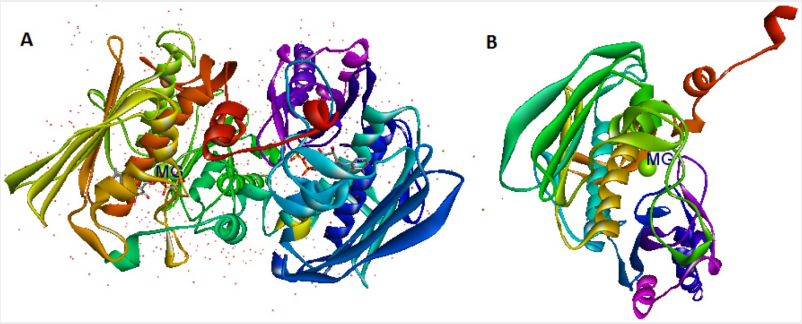

The molecular docking between synthesized ligands and the 1ZXM receptor was executed to define the appropriate conformation of each ligand in the receptor and the secondary forces resulting between the active amino acids of the receptor and ligand. The protein was kept in a rigid conformation whilst the ligand was in flexible conformation. The best conformations of the ligands were analyzed for their binding interactions and were evaluated by binding free energies (S-score, Kcal/mol), and bonds interactions between ligand atoms and active site residues.

It was established that among the different docking conformations of compounds, **4r** is shown as the highest docking scores −8.9 Kcal/mol compared to **4p** and **4q** (-8.2 Kcal/mol) as well as the standard anticancer drug Adriamycin (Table 4), this due to the OCH_3 interaction, and π-Alkyl interactions, also to conventional hydrogen bonding

interactions with active pocket of topoisomerase-II enzyme.

Note: The table layout displayed in 'Edit' view is not how it will appear in the printed/pdf version. This html display is to enable content corrections to the table. To preview the printed/pdf presentation of the table, please view the 'PDF' tab.

Table 4. Binding scores and the non-bonding interactions of 4p, 4q, 4r and the ADM with amino acid residues of 1ZXM.

Compounds	Docking score (Kcal/ mol)	Amino acid with hydrogen bonding interaction	N hydrogen bonding interaction [distance (Å)]	Hydrophobic interaction [distances (Å)]	Residues of binding site
4p	–8.2	Ser 149 Asn 95	1 (2.46) 1 (3.51)	Ala 167: Pi alkyl (4.69) Ile 217: Alkyl (4.52) Ale 118 : Alkyl (5.34) Thr 215 : Pi-Sigma Ile 141: Pi alkyl (5.06) Ale 88 : Alkyl (5.36)	Ala 92, Ala 167, Ser 149, Asn 120, Asn 95, Ile 88, Ile 118, Ile 217, Ile 141, Thr 215
4q	–8.2	Ser 149	1 (2.45)	Ile 88 : Alkyl (5.45) Ala 167 : alkyl (4.18) Ala 167 : Pi-alkyl (4.77)	Asn 120, Ala 92, Ile 88, Ile 118, Ile 217, Ala 167, Ser 149
4r	–8.9	Gly 164 Tyr 165 Asn 150 Ser 149 Ala 92	1 (2.32) 1 (1.97) 1 (2.71) 1 (1.73) 1 (3.24)		Gly 164, Tyr 165, Asn 91, Asn 120, Ala 92, Asn 150, Ser 149
Adriamycin (ADM)	–8.0	Asn 91 Ser 149 Ser 149 Ser 148 His 130	1 (3.55) 1 (2.29) 1 (2.31) 1 (3.07) 1 (2.77)	Ser 149 : Pi-sigma (3.79) Ile 125: Pi alkyl (5.05) Ile 125: Pi alkyl (5.43) Ile 141: Pi-sigma (3.67) Ile 141: Pi-sigma (3.41) His 130: Pi alkyl (5.01) His 137: Pi alkyl (5.48)	Asn 91, Ser 148, Ser 149, Ile, 125, Ile 141, Leu 140, His 130, Val 137

Place the cursor position on table column and click "Add New" to add table footnote.

As shown in Figure 7 and detailed in Table 4, only the ligand **4r** has a direct interaction with the center of the Mg^{+2}:309 metal, the distance of this electrostatic interaction was 2.65 Å.

Figure 7. The docked 2D and 3D images of **4p**, **4q** and **4r** compounds and commercial drug Adriamycin with 1ZXM receptor.

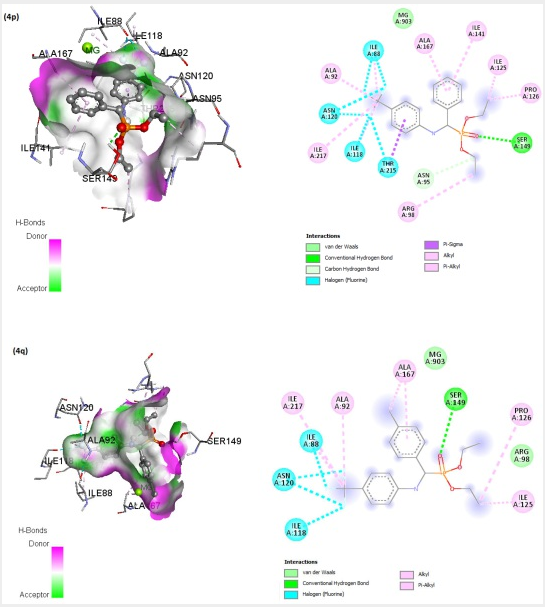

Furthermore, the ADM binds to 1ZXM receptor through various interactions, including Pi-sigma, Alkyl and Pi-Alkyl interactions as well as conventional hydrogen bond with Asn 91, Ser 148 and His 130. Those residues were identified in the active site that drives the enzymatic activity of the 1ZXM. The three ligands have a common hydrogen bond interaction with the Ser 149. The stability of the docked ligand **4r** is due exclusively to the hydrogen bond interactions between the -OCH_3 and the P = O moieties to the binding site of the receptor. However, for the structures **4p** and **4q** as well as the ADM, their stability was supported by the presence of hydrophobic interactions. It has been reported that the binding affinity and drug efficacy associated with hydrophobic interactions can be optimized by incorporating them at the site of the hydrogen bonding (Patil et al., 2010). Finally, taken in account a number of hydrogen binding to the site active residues and the binding energy score, the compound **4r** shows as the most stable and presents a high affinity to the protein receptor.

3.4. ADMET prediction and drug likeness

3.4.1. Absorption and physicochemical properties

The drug-likness properties and potential toxicity risk as well as the physicochemical properties were predicted using Swiss-ADME server. In the present study, the ADMET prediction of the α-aminophosphonates **4p**, **4q** and **4r** are treated and summarized in two Tables 4 and 5. A comparison with commercial drug Adriamycin (ADM) was chosen for their anti-proliferation activities cytotoxicity activity against three types of human cancer cell lines, breast cancer, prostate cancer and stomach cancer cells (Jing-Zi et al., 2010).

Note: The table layout displayed in 'Edit' view is not how it will appear in the printed/pdf version. This html display is to enable content corrections to the table. To preview the printed/pdf presentation of the table, please view the 'PDF' tab.

Table 5. The physicochemical properties of designed molecules for drug-likeness Pre-diction based on Lipinski's rule of five.

Physicochemical properties	ADM	4p	4q	4r
Molecular weight g/mol	543.52 g/mol	387.33 g/mol	421.78 g/mol	405.47 g/mol
NHBA	12	6	6	4
NHBD	6	1	1	1
Consensus Log P_{Ow}	0.44	4.37	4.92	4.59
Log S	–3.46	–6.92	–7.50	–7.35
TPSA (Å)2	206.07	57.37	57.37	66.60

Place the cursor position on table column and click "Add New" to add table footnote.

Based on the physicochemical properties with their ranges as described the Lipinski's rule of five, a violation of those rules was examined for the **ADM** compared to the synthesized α-aminophosphonates (**4p**, **4q** and **4r)**. The results show no violation of the rules for **4p**, **4q** and **4r,** they have a molecular weight are less than 500 Da, which suggests that they can move easily across biological membranes. In addition, these molecules were well tolerated by cell membranes and this is confirmed by their log *p* value (<5). The total polar surface area (TPSA) it is a stronger indicator of whether molecule is orally active or not. All molecules synthesized are respect the rule of the TPSA ($\leq$140 $Å^2$) which indicates that they have a high oral biovailability, compared to Adriamycin having (TPSA = 206.07 $Å^2$). Table 5.

Moreover, the oral bioavailability radar of compounds is very important for analyzing the drug-likeness of a molecule and defining its pharmacological potential, by taking into consideration the six physicochemical properties such as; lipophilicity (lipo), size, polarity (polar), insolubility (insolu), flexibility (flex) and unsaturation (insatu) (Arulraj et al., 2022a; 2022b). Consequently, the oral bioavailability radar show that all synthesized molecules fall entirely inside the pink area representing the optimal range of the mentioned descriptors, thus indicating that the studied molecules could be considered druglike (Figure 8**)**.

Figure 8. Biovailability radars and physicochemical properties of Adriamycin, **4p**, **4q** and **4r**.

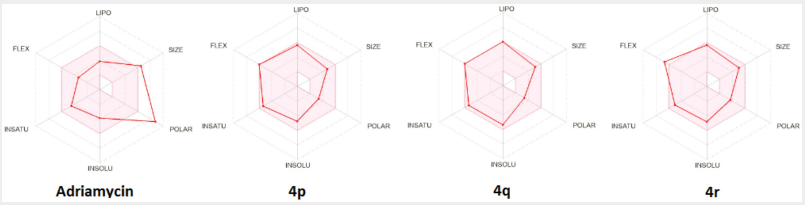

Further, one of the fast and efficient approaches to examine molecules for the human blood-brain barrier (BBB) penetration and gastrointestinal absorption (GIA) is the BOILED-Egg method, which is derived from lipohilicity and polarity (Daina & Zoete, 2016). As such, points in the Egg's yolk correspond to molecules predicted to passively permeate through the BBB and white correspond to molecules predicted to be passively absorbed by the gastrointestinal absorption (GIA) (Figure 9). Furthermore, molecules found to be effluated (PGP+) and not to be effluated (PGP-) from the central nervous system by the P-glycoprotein are shown as blue and red dots, respectively. According to the results, none of the synthesized molecules displayed permeation through the blood-brain barrier, whereas all were predicted to be passively absorbed by the gastrointestinal property with the PGP + for **4p** and **4r**, and with the PGP- for **4q** compared to Adriamycin, which is out of range.

Figure 9. Overview of the BOILED-Egg construction for designed molecules **4p**, **4q**, **4r** and **ADM** from the SwissADME online sever.

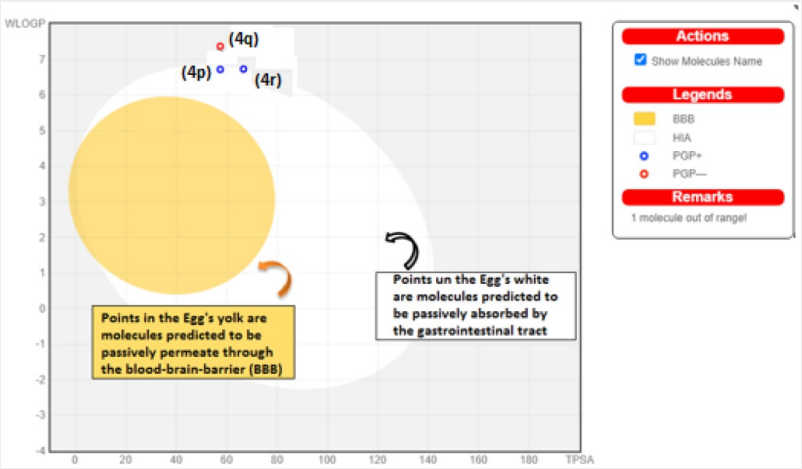

3.4.2. Distribution, metabolism and pharmacokinetic properties

Pharmacokinetic properties are another important indicator of the likelihood of therapeutic success for drug molecules like these potential inhibitors. High GI absorption denotes that the compound could be better absorbed from the intestinal tract upon oral administration. It is noted that **4p** and **4r** exhibit high GI absorption compared to ADM and **4q** compounds which exibit low GI absorption, however it was found to be unable to cross the blood-brain barrier (BBB) partition, is depicted in Table 6.

Note: The table layout displayed in 'Edit' view is not how it will appear in the printed/pdf version. This html display is to enable content corrections to the table. To preview the printed/pdf presentation of the table, please view the 'PDF' tab.

Table 6. Predicted pharmacokinetic and drug-likeness properties of ADM, 4p, 4q and 4r.

Pharmacokinetics properties	ADM	4p	4q	4r
GI absorption	Low	High	Low	High
BBB permeant	No	No	No	No
P-gp substrate	Yes	Yes	No	Yes
CYP1A2 inhibitor	No	No	No	No
CYP2C19 inhibitor	No	Yes	Yes	Yes
CYP2C9 inhibitor	No	Yes	Yes	Yes
CYP2D6 inhibitor	No	Yes	Yes	Yes
CYP3A4 inhibitor	No	Yes	Yes	Yes
Log K_p (skin permeation)	–8.71 cm/s	–5.54 cm/s	–5.31 cm/s	–5.12 cm/s

GI absorption: gastrointestinal absorption; BBB: blood–brain barrier; CYP: Cytochrome P450; P-gp substrate: glycoprotein substrate P.

In predicting, the efflux by p-glycoprotein, only **4q** comes out as the substrate. In fact, it was reported that a given molecule could more likely take part in Drug-Drug Interactions (DDI) with other active molecules if it inhibits more CYP enzymes (Cheng et al., 2011), especially the isoforms (CYP1A2, CYP2C19, CYP2C9, CYP2D6 and CYP3A4) which are responsible of 90% for oxidative metabolic reactions (Williams et al., 2004). Therefore, all compounds were predicted to show no potency against CYP1A2, and are inhibitors of at least of all the CYP450 isoforms (CYP2C19, CYP2C9, CYP2D6 and CYP3A4) except ADM. Skin sensitization is a safety assessment indicator that provides information on a compound's ability to induce skin allergy when administered (Alves et al., 2015), the studied molecules (**ADM, 4p**, **4q**, **4r)** show low skin permeability at −8.71 cm/s, −5.54 cm/s, −5.31 cm/s and −5.12 cm/s respectively. Here, the results proved that these compounds are harmless and cure for skin allergies (Abdelrheem et al., 2021; Kavitha & Alivelu, 2021).

3.4.3. Drug-likeness and bioavailability

Drug-likeness is defined by rules that evaluate qualitatively the chance for a given molecule to become a possible oral drug with respect to its bioavailability by considering ranges of specific physicochemical properties (Daina et al., 2017). Veber's rule shows non-violation for all synthesized products (**4p**, **4q** and **4r**). Egan's rule is verified only by **4r**. Mugge's rule indicates that **4p** can be considered as good drugs. Based on these results, it can be concluded that the studied compounds have to potential to become excellent drug candidates (Table 7).AQ5

Note: The table layout displayed in 'Edit' view is not how it will appear in the printed/pdf version. This html display is to enable content corrections to the table. To preview the printed/pdf presentation of the table, please view the 'PDF' tab.

Table 7. Drug-likeness profile and medicinal properties calculated for the studied molecule.

Drug-likeness	ADM	4p	4q	4r
Lipinski	No	Yes	Yes	Yes
Ghose	No	No	No	No
Veber	No	Yes	Yes	Yes
Egan	No	No	No	Yes
Muegge	No	Yes	No	No
Bioavailability score	0.17	0.55	0.55	0.55
Synthetic accessibility (SA)	5.81	4.05	4.02	4.37

Place the cursor position on table column and click 'Add New' to add table footnote.

4. Conclusion

In conclusion, we have developed a sustainable and an eco-friendly methodology for the preparation of α-aminophosphontates derivatives **(4a-r)** using 2-hydroxymethyl-18-crown-6 as an efficient homogeneous organocatalyst. This new catalytic multicomponent reaction using 5 mol% has number of advantages; including a substantial preparation of organophosphorus compounds under environmental friendliness transition metal-free conditions and short reaction time. Three structures of CF_3 derivatives (**4p, 4q** and **4r**) were selected and optimized by the DFT/CAM-B3LYP/6-31G (d,p) calculations to reveal its geometrical parameters and electronic properties. The HOMO and LUMO are mainly delocalized over the aromatic ring and the amino group, while the LUMO is mainly spread over the CF_3 fragment. HOMO and LUMO energy gaps justify the eventual charge transfer interactions taking place within the molecules. The molecular electrostatic potential has been mapped for predicting sites of electrophilic and nucleophilic attack, we have mentioned that the negative possible positions are about electronegative atoms (N and O) and the conjugated double bonds, and the positive possible zones are about the hydrogen atoms. In *silico* docking study showed that the docked conformations also formed an H-bonding interaction within the active site of enzyme. The three ligands **4p, 4q** and **4r** have shown potent hydrogen bonding interactions with active site of topoisomerase-II enzyme as Adriamycin. Depending on the results, only the ligand **4r** has a direct electrostatic interaction with the center of the Mg^{+2}:309 metal, it has the highest score energy (-8.9 Kcal/mol) and is deeply fitted the active pocket of the enzyme forming five hydrogen bond interactions, which reflects high stability and affinity of this molecule to the receptor. However, for the structures **4p** and **4q** as well as the Adriamycin, their stability was supported by the presence of hydrophobic interactions. In addition, the synthesized compounds (**4p, 4q** and **4r**) were examined for their potential as drugs using Lipinski's five rules and ADMET studies compared to Adriamycin, the results confirm the success of these potential inhibitors as candidates in drug discovery, which may have an influence in anticancer activity. Drug-likeness of designed compounds is analyzed by oral bioavailability radar and show their high pharmacological potential.

Acknowledgments

The Algerian Ministry of Education and Scientific Research (DGRSDT, FNR) is gratefully acknowledged for financial support of this work. The technical support provided by Emilie KOLODZIEJ is highly appreciated.

Disclosure statement

The authors declare that they have no known competing financial interests or personal relationships that could have appeared to influence the work reported in this paper.

Note: this Edit/html view does not display references as per your journal style. There is no need to correct this. The content is correct and it will be converted to your journal style in the published version.

References

Aissa, R., Guezane-Lakoud, S., Gali, L., Toffano, M., Ignaczak, A., Adamiak, M., Merabet-Khelassi, M., Guillot, R., & Aribi-Zouioueche, L. (2022). New promising generation of phosphates α-aminophosphonates: Design, Synthesis, In-vitro biological evaluation and Computational study. *Journal of Molecular Structure*, *1247*(17), 131336. https://doi.org/10.1016/j.molstruc.2021.131336

Aissa, R., Guezane-Lakoud, S., Kolodziej, E., Toffano, M., & Aribi-Zouioueche, L. (2019). Diastereoselective synthesis of bis(a-aminophosphonates) by lipase catalytic promiscuity. *New Journal of Chemistry*, *43*(21), 8153–8159. https://doi.org/10.1039/C8NJ06235H

Aissa, R., Guezane-Lakoud, S., Toffano, M., Gali, L., & Aribi-Zouioueche, L. (2021). Fiaud's acid, a novel organocatalyst for diastereoselective bis α-aminophosphonates synthesis with *in-vitro* biological evaluation of antifungal, antioxidant and enzymes inhibition potential. *Bioorganic & Medicinal Chemistry Letters*, *41*(1), 128000.

https://doi.org/10.1016/j.bmcl.2021.128000

Asiri, A. M., Karabacak, M., Kurt, M., & Alamry, K. A. (2011). Synthesis, molecular conformation, vibrational and electronic transition, isometric chemical shift, polarizability and hyperpolarizability analysis of 3-(4-Methoxy-phenyl)-2-(4-nitro phenyl)-acrylonitrile: A combined experiment and theoretical analysis. *Spectrochimica Acta. Part A, Molecular and Biomolecular Spectroscopy*, *82*(1), 444–455. https://doi.org/10.1016/j.saa.2011.07.076

Arulraj, R., Nurulhuda, M., Wee Joo, C., Mouna, M., Sivakumar, S., & Noureddine, I. (2022a). 3-Chloro-3-methyl-2,6-diarylpiperidin-4-ones as anti-cancer agents: Synthesis, biological evaluation, molecular docking, and in silico ADMET prediction. *Biomolecules*, *12*(8), 1093. https://doi.org/10.3390/biom12081093

Arulraj, R., Ahlam Roufieda, G., Sivakumar, S., Anitha, K., Rajkumar, K., Nourdine, B., Abdelkader, C., & Manikandan, E. (2022b). Synthesis, vibrational spectra, Hirshfeld surface analysis, DFT calculations, and in silico ADMET study of 3-(2-chloroethyl)-2,6-bis(4-fluorophenyl)piperidin-4-one: A potent anti-Alzheimer agent. *Journal of Molecular Structure*, *1269*, 133845. https://doi.org/10.1016/j.molstruc.2022.133845

Alves, V. M., Muratov, E., Fourches, D., Strickland, J., Kleinstreuer, N., Andrade, C. H., & Tropsha, A. (2015). Predicting chemically-induced skin reactions. Part II: QSAR models of skin permeability and the relationships between skin permeability and skin sensitization. *Toxicology and Applied Pharmacology*, *284*(2), 262–272. https://doi.org/10.1016/j.taap.2014.12.013

Abdelrheem, D. A., Rahman, A. A., Elsayed, N. M., Abd El-Mageed, H. R., Mohamed, H. S., & Ahmed, S. A. (2021). Isolation, characterization, in vitro anticancer activity, DFT calculations, molecular docking, bioactivity score, drug-likeness and admet studies of eight phytoconstituents from brown alga sargassum platycarpum. *Journal of Molecular Structure*, *1225*, 129245. https://doi.org/10.1016/j.molstruc.2020.129245

Abraham, C. S., Prasana, J. C., & Muthu, S. (2017). Quantum mechanical, spectroscopic and docking studies of 2-amino-3-bromo-5-nitropyridine by density functional method. *Spectrochimica Acta. Part A, Molecular and Biomolecular Spectroscopy*, *181*, 153–163. https://doi.org/10.1016/j.saa.2017.03.045

Aita, S., Badavath, V. N., Gundluru, M., Sudileti, M., Nemallapudi, B. R., Gundala, S., Zyryanov, G. V., Chamarti, N. R., & Cirandur, S. R. (2021). Novel α-aminophosphonates of imatinib Intermediate: Synthesis, anticancer Activity, human Abl tyrosine kinase Inhibition, ADME and toxicity prediction. *Bioorganic Chemistry*, *109*, 104718. https://doi.org/10.1016/j.bioorg.2021.104718

Bonarska, D., Kleszczynska, H., & Sarapuk, J. (2002). Antioxidative activity of some phenoxy and organophosphorous compounds. *Cellular & Molecular Biology Letters*, *7*(3), 929–935.

Becke, A. D. (1993). Density-functional thermochemistry III. The role of exact exchange. *The Journal of Chemical Physics*, *98*(7), 5648–5652. https://doi.org/10.1063/1.464913

Cinquini, M., & Tundo, P. (1976). Synthesis of alkyl-substituted crown ethers: efficient phase-transfer catalysts. *Synthesis*, *1976*(08), 516–519. https://doi.org/10.1055/s-1976-24101

Chung-Kiak, P., & Han-Ping, D. S. (2016). Density functional based tight binding (DFTB) study on the thermal evolution of amorphous carbon. *Graphene*, *5*, 51–54. https://doi.org/10.4236/graphene.2016.52006

Cytlak, T., Kaźmierczak, M., Skibińska, M., & Koroniak, H. (2017). Latest achievements in the preparation of fluorinated aminophosphonates and aminophosphonic acids. *Phosphorus, Sulfur, and Silicon and the Related Elements*, *192*(6), 602–620. https://doi.org/10.1080/10426507.2017.1287706

Cheng, F., Yu, Y., Shen, J., Yang, L., Li, W., Liu, G., Lee, P. W., & Tang, Y. (2011). Classification of cytochrome P450 inhibitors and noninhibitors using combined classifiers. *Journal of Chemical Information and Modeling*, *51*(5), 996–1011. https://doi.org/10.1021/ci200028n

Dennington, R., Keith, T., Millam, J., & Inc, S. (2009). V.5. GaussView.

Dix, J. P., Wittenbrink-Dix, A., & Vögtle, F. (1980). Ion-selective steering of the reaction rate and of the catalyst activity by crown-ether complexation. *Naturwissenschaften*, *67*(2), 91–93. https://doi.org/10.1007/BF01054694

Daina, A., Michielin, O., & Zoete, V. (2017). SwissADME: A free web tool to evaluate pharmacokinetics, drug-likeness and medicinal chemistry friendliness of small molecules. *Scientific Reports*, *7*, 42717. https://doi.org/10.1038/srep42717

Domingo, L. R., Aurell, M. J., Pérez, P., & Contreras, R. (2002). Quantitative characterization of the global electrophilicity power of common diene/dienophile pairs in Diels-Alder reactions. *Tetrahedron*, *58*(22), 4417–4423. https://doi.org/10.1016/S0040-4020(02)00410-6

Daina, A., & Zoete, V. (2016). A BOILED-egg to predict gastrointestinal absorption and brain penetration of small molecules. *ChemMedChem*. *11*(11), 1117–1121. https://doi.org/10.1002/cmdc.201600182

Elfily, A. A. (2020). Ribavirin, sofosbuvir remdesivir, galidesivir, and tenofovir against SARS-Cov-2 RNA dependent RNA polymerase (RdRp): A molecular docking study . *Life Sciences*, *253*, 117592. https://doi.org/10.1016/j.lfs.2020.117592

Ferrah, M., Samia, G.-L., Bendjeffal, H., Aissa, R., Merabet-Khelassi, M., Toffano, M., & Aribi-Zouioueche, L. (2022). Full factorial optimization of α-aminophosphonates synthesis using diphenylphosphinic acid as efficientorganocatalyst. *Reaction Kinetics, Mechanisms and Catalysis*. https://doi.org/10.1007/s11144-022-02329-0

Frisch, M. J., Trucks, G. W., Schlegel, H. B., Scuseria, G. E., Robb, M. A., Cheeseman, J. R., Scalmani, G., Barone, V., Mennucci, B., Petersson, G. A., Nakatsuji, H., Caricato, M., Li, X., Hratchian, H. P., Izmaylov, A. F., Bloino, J., Zheng, G., Sonnenberg, J. L., Hada, M., … Gaussian, D. J. (2009). *09, Revision A.02*. Gaussian, Inc.

Feng, L., Yang, H., Cui, X., Chen, D., & Li, G. (2018). Experimental and theoretical investigation on corrosion inhibitive properties of steel rebar by a newly designed environmentally friendly inhibitor formula. *RSC Advances*, *8*(12), 6507–6518. https://doi.org/10.1039/C7RA13045G

Grzywa, R., & Sieńczyk, M. (2013). Phosphonic esters and their application of protease control. *Current Pharmaceutical Design*, *19*(6), 1154–1178. https://doi.org/10.2174/1381612811319060014

Guezane-Lakoud, S., Lecouvey, M., Berrebah, H., & Aouf, N. E. (2015). Synthesis of chiral phosphonoacetamides and their toxic effects on Paramecium sp. *Organic Communications*, *8*, 1–8.

Guezane-Lakoud, S., Toffano, M., & Aribi-Zouioueche, L. (2017). Promiscuous lipase catalyzed a new P–C bond formation: Green and efficient protocol for one-pot synthesis of α-aminophosphonates. *Heteroatom Chemistry*, *28*(6), e21408. https://doi.org/10.1002/hc.21408

Heydari, A., Hamadi, H., & Pourayoubi, M. (2007). A new one-pot synthesis of α-amino phosphonates catalyzed by $H_3PW_{12}O_{40}$. *Catalysis Communications*, *8*(8), 1224–1226. https://doi.org/10.1016/j.catcom.2006.11.008

Hyun, M. H. (2012). Chromatographic separations and analysis: Chiral crown ether-based chiral stationary phases. In E. M. Carreira & H. Yamamoto (Eds.), *Comprehensive chirality* (Vol. 8, pp. 263–285). ISBN 9780080951683 Elsevier. https://doi.org/10.1016/B978-0-08-095167-6.00827-2

Jing-Zi, L., Bao-An, S., Hui-Tao, F., Pinaki, S. B., Wen-Ting, W., Song, Y., Weiming, X., Jian, W., Lin-Hong, J., Xue, W., De-Yu, H., & Song, Z. (2010). Synthesis and *in vitro* study of pseudo-peptide thioureas containing α-aminophosphonate moiety as potential antitumor agents. *European Journal of Medicinal Chemistry*, *45*(11), 5108–5112. https://doi.org/10.1016/j.ejmech.2010.08.021

Kohn, W., & Sham, L. J. (1965). Quantum density oscillations in an inhomogeneous electron gas. *Physical Review*, *137*(6A), A1697–A1705. https://doi.org/10.1103/PhysRev.137.A1697

Kandula, M. K. R., Shaik, M. S., Nagaripati, S., Kotha, P., Bakthavatchala, R., Sravya, G., Grigory, Z., & Cirandur, S. R. (2017). One-pot green synthesis and cytotoxicity of new α-aminophosphonates. *Research on Chemical Intermediates*, *43*(12), 7087–7103. https://doi.org/10.1007/s11164-017-3060-y

Kosar, B., & Albayrak, C. (2011). Spectroscopic investigations and quantum chemical computational study of (E)-4-methoxy-2-[(p-tolylimino) methyl phenyl]. *Spectrochimica Acta. Part A, Molecular and Biomolecular Spectroscopy*, *78*(1), 160–167. https://doi.org/10.1016/j.saa.2010.09.016

Kavitha, N., & Alivelu, M. (2021). Investigation of structures, QTAIM, RDG, ADMET, and docking properties of SASC compound using experimental and theoretical approach. *Computational and Theoretical Chemistry*, *1201*, 113287. https://doi.org/10.1016/j.comptc.2021.113287

Kerkour, R., Chafai, N., Moumeni, O., & Chafaa, S. (2023). Novel α-aminophosphonates derivates synthesis, theoretical calculation, Molecular docking, and in silico prediction of potential inhibition of SARS-CoV-2. *Journal of Molecular Structure*, *1272*, 134196. https://doi.org/10.1016/j.molstruc.2022.134196

Lakoud, S. G., Merabet-Khelassi, M., & Aribi-Zouioueche, L. (2016). $NiSO_4$-$6H_2O$ as a new, efficient, and reusable catalyst for the α-aminophosphonates synthesis under mild and eco-friendly conditions. *Research on Chemical Intermediates*, *42*(5), 4403–4415. https://doi.org/10.1007/s11164-015-2283-z

Laschat, S., & Kunz, H. (1992). Carbohydrates as chiral templates: Stereoselective synthesis of *(R)*- and *(S)*-α-aminophosphonic acid derivatives. *Synthesis*, *1992*(1/2), 90–95. https://doi.org/10.1055/s-1992-34155

Lamb, J. D., Izatt, R. M., & Christensen, J. J. (1981). In R. M. Izatt and J. J. Christensen (Eds.), *Progress in macrocyclic chemistry* (Vol. 2, pp. 41–90). Jhon Wiley & Sons.

Liittringhaus, A. (1937). Hydroquinone or 1.5 and 1.6 dihydroxynaphtalemen cyclic polyethers. *Justus Liebigs Annalen Der Chemie*, *528*, 181–210. https://doi.org/10.1002/jlac.19375280112

Luo, Y., Ouyang, G., Tang, Y., Y-M, H., & Q-H, F. (2020). Diaza-crown ether-bridged chiral diphosphoramidite ligands: Synthesis and applications in asymmetric catalysis. *The Journal of Organic Chemistry*, *85*(12), 8176–8184. https://doi.org/10.1021/acs.joc.0c00223

Lipinski, C. A. (2016). Rule of five in 2015 and beyond: Target and ligand structural limitations, ligand chemistry structure and drug discovery project decisions. *Advanced Drug Delivery Reviews*, *101*, 34–41. https://doi.org/10.1016/j.addr.2016.04.029

Maier, L. (1990). Organic phosphorus compounds 91.[1]synthesis and properties of 1-amino-2-arylethylphosphonic and-phosphinic acids as well as -phosphine oxides. *Phosphorus, Sulfur, and Silicon and the Related Elements*, *53*(1-4), 43–67. https://doi.org/10.1080/10426509008038012

Maier, L., & Diel, P. J. (1991). Organic phosphorus compounds 94 preparation, physical and biological properties of amino-arylmethylphosphonic- and-phosphonous acids. *Phosphorus, Sulfur, and Silicon and the Related Elements*, *57*(1-2), 57–64. https://doi.org/10.1080/10426509108038831

Mcdowell, W. J. (1988). Crown ethers as solvent extraction reagents: Where do we stand? *Separation Science and Technology*, *23*(12-13), 1251–1268. https://doi.org/10.1080/01496398808075628

Mekky, A. H., Hlhaes, H. G., El-Okr, M. M., Al-Aboudi, A. S., & Ibrahim, M. A. (2015). Effect of solvents on the electronic properties of fullerene base systems: Molecular modelling. *Journal of Computational and Applied Mathematics*, *4*(1), 1–4. https://doi.org/10.4172/2168-9679.1000203

Merabet, M., Melais, N., Boukachabia, M., Fiaud, J. C., & Zouioueche-Aribi, L. (2007). Effet d'un ether couronne sur le systeme catalytique dans la reaction d'acylation du 1-acenaphtenol avec la lipase de candida cylindracea. *Journal De la Société Algerienne De Chimie*, *17*(2), 185–194.

Morris, G. M., Huey, R., Lindstrom, W., Sanner, M. F., Belew, R. K., Goodsell, D. S., & Olson, A. J. (2009). AutoDock4 and AutoDockTools4: Automated Docking with Selective Receptor Flexiblity. *Journal of Computational Chemistry*, *30*(16), 2785–2791. https://doi.org/10.1002/jcc.21256

Mirzaei, M., Hossein, E., Bagherjeri, F. A., Mirzaei, M., & Farhadipour, A. (2018). Investigation of non-covalent and hydrogen bonding interactions on the formation of crystalline networks and supramolecular synthons of series of α-aminophosphonates: Cristallography and DFT studies. *Journal of Molecular Structure*, *1163*, 316–326. https://doi.org/10.1016/j.molstruc.2018.03.014

Mucha, A., Kafarski, P., & Berlicki, Ł. (2011). Remarkable potential of the α-aminophosphonate/phosphinate structural motif in medicinal chemistry. *Journal of Medicinal Chemistry*, *54*(17), 5955–5980. https://doi.org/10.1021/jm200587f

Nagayama, S., & Kobayashi, S. (2000). A novel chiral lead (II) catalyst for enantioselective aldol reactions in aqueous media. *Journal of the American Chemical Society*, *122*(46), 11531–11532. https://doi.org/10.1021/ja0012341

Omichi, M., Yamashita, S., Okura, Y., Ikutomo, R., Ueki, Y., Seko, N., & Kakuchi, R. (2019). Surface engineering of fluoropolymer films via the attachment of crown ether derivatives based on the combination of radiation-induced graft polymerization and the *Kabachnik–Fields* reaction. *Polymers*, *11*(8), 1337. https://doi.org/10.3390/polym11081337

Olasupo, S. B., Uzairu, A., Shallangwa, G. A., & Uba, S. (2020). Profiling the antidepressant properties of phenyl piperidine derivatives as inhibitors of serotonin transporter (SERT) via cheminformatics modeling, molecular docking and ADMET predictions. *Scientific African*, *9*, e00517. https://doi.org/10.1016/j.sciaf.2020.e00517

Oleg, T., & Olson, A. J. (2010). AutoDock Vina: Improving the speed and accuracy of docking with a new scoring function, efficient optimization, and multithreading. *Journal of Computational Chemistry*, *31*, 254–261. https://doi.org/10.1002/jcc.21334

Pan, W., Ansiaux, C., & Vincent, S. P. (2007). Synthesis of acyclic galactitol-and lyxitol-aminophosphonates as inhibitors of UDP-galactopyranose mutase. *Tetrahedron Letters*, *48*(25), 4353–4356. https://doi.org/10.1016/j.tetlet.2007.04.113

Patil, R., Das, S., Stanley, A., Yadav, L., Sudhakar, A., & Varma, A. K. (2010). Optimized hydrophobic interactions and hydrogen bonding at the target-ligand interface leads the pathways of drug-designing. *PloS One*, *5*(8), e12029. https://doi.org/10.1371/journal.pone.0012029

Pedersen, C. J. (1967). Cyclic polyethers and their complexes with metal salts. *Journal of the American Chemical Society*, *89*(10), 2495–2496. https://doi.org/10.1021/ja00986a052

Pedersen, C. J. (1970). Crystalline Salt Complexes of Macrocyclic Polyethers. *Journal of the American Chemical Society*, *92*, 386–391. https://doi.org/10.1021/ja00705a605

Pham, T. S., Czirok, J. B., Balazs, L., Pal, K., Kubinyi, M., Bitter, I., & Jaszay, Z. (2011). BINOL-based azacrown ether catalyzed enantioselective Michael addition: Asymmetric synthesis of α-aminophosphonates. *Tetrahedron: Asymmetry*. *22*(4), 480–486. https://doi.org/10.1016/j.tetasy.2011.02.002

Rostamnia, S., & Doustkhah, E. (2015). Synthesis of water-dispersed magnetic nanoparticles (H_2O-DMNPs) of *β*-cyclodextrin modified Fe_3O_4 and its catalytic application in Kabachnik–Fields multicomponent reaction. *Journal of Magnetism and Magnetic Materials*, *386*, 111–116. https://doi.org/10.1016/j.jmmm.2015.03.064

Rostamnia, S., & Amini, M. (2014). Ultrasonic and Lewis acid ionic liquid catalytic system for Kabachnik–Fields reaction. *Chemical Papers*, *68*(6), 834–837. https://doi.org/10.2478/s11696-013-0516-4

Raafat, M., Mohamed, I. A., & Faten, M. K. A. (2008). Quantum chemical studies on the inhibition of corrosion of copper surface by substituted uracils. *Applied Surface Science*, *255*, 2433–2441. https://doi.org/10.1016/j.apsusc.2008.07.155

Schug, K. A., & Lindner, W. (2005). Noncovalent binding between guanidinium and anionic groups: Focus on biological- and synthetic-based arginine/guanidinium interactions with phosph[on]ate and sulf[on]ate residues. *Chemical Reviews*, *105*(1), 67–114. https://doi.org/10.1021/cr040603j

Satish, U. D., Kiran, R., Kharat, A. R., Yadav, S. U. S., Manoj, G. D., Jaiprakash, N. S., & Rajendra, P. P. (2018). Synthesis of novel α-aminophosphonate derivatives, biological evaluation as potent antiproliferative agents and molecular docking. *ChemistrySelect*, *3*(20), 5552–5558. https://doi.org/10.1002/slct.201800798

Sivala, M. R., Devineni, S. R., Golla, M., Medarametla, V., Pothuru, G. K., & Chamarthi, N. R. (2016). A heterogeneous catalyst, SiO_2-$ZnBr_2$: An efficient neat access for α-aminophosphonates and antimicrobial activity evaluation. *Journal of Chemical Sciences*, *128*(8), 1303–1313. https://doi.org/10.1007/s12039-016-1113-1

Turcheniuk, K. V., Kukhar, V. P., Roschenthaler, G. V., Acena, J. L., Soloshonok, V. A., & Sorochinsky, A. E. (2013). Recent advances in the synthesis of fluorinated aminophosphonates and aminophosphonic acids. *RSC Advances*, *3*(19), 6693–6716. https://doi.org/10.1039/c3ra22891f

Uparkar, J. J., Dhavan, P. P., Jadhav, B. L., & Pawar, S. D. (2022). Design, synthesis and biological evaluation of furan based α-aminophosphonate derivatives as anti-Alzheimer agent. *Journal of the Iranian Chemical Society*, *19*(7), 3103–3116. https://doi.org/10.1007/s13738-022-02515-w

Vahda, S. M., Baharfar, R., Tajbakhsh, M., Heydari, A., Baghbanian, S. M., & Khaksar, S. (2008). Organocatalytic synthesis of α-hydroxy and α-aminophosphonates. *Tetrahedron Letters*, *49*(46), 6501–6504. https://doi.org/10.1016/j.tetlet.2008.08.094

Wei, H., Ruthenburg, A. J., Bechis, S. K., & Verdine, G. L. (2005). Nucleotide-dependent domain movement in the ATPase domain of a human type IIA DNA topoisomerase. *The Journal of Biological Chemistry*, *280*(44), 37041–37047. https://doi.org/10.1074/jbc.M506520200

Williams, J. A., Hyland, R., Jones, B. C., Smith, D. A., Hurst, S., Goosen, T. C., Peterkin, V., Koup, J. R., & Ball, S. E. (2004). Drug-drug interactions for UDP-glucuronosyltransferase substrates: A pharmacokinetic explanation for typically observed low exposure (AUCi/AUC) ratios. *Drug Metabolism and Disposition: The Biological Fate of Chemicals*, *32*(11), 1201–1208. https://doi.org/10.1124/dmd.104.000794

Xavier, S., & Periandy, S. (2015). Spectroscopic (FT-IR, FT-Raman, UV and NMR) investigation on 1-phenyl-2-nitropropene by quantum computational calculations. *Spectrochimica Acta. Part A, Molecular and Biomolecular Spectroscopy*, *149*, 216–230. https://doi.org/10.1016/j.saa.2015.04.055

Yadav, J. S., Reddy, B. V. S., Raj, K. S., Reddy, K. B., & Prasad, A. R. (2001). Zr^{4+}catalyzed efficient synthesis of α-aminophosphonates. *Synthesis*, *2001*(15), 2277–2280. https://doi.org/10.1055/s-2001-18444

Yanai, T., Tew, D., & Handy, N. (2004). New hybrid exchange-correlation functional using the Coulomb attenuating method (CAM-B3LYP). *Chemical Physics Letters*, *393*(1-3), 51–57. https://doi.org/10.1002/chir.22384

Author Query

1. **Query** [AQ0] : Please review the table of contributors below and confirm that the first and last names are structured correctly and that the authors are listed in the correct order of contribution. This check is to ensure that your names will appear correctly online and when the article is indexed.

Sequence	Prefix	Given name(s)	Surname	Suffix
1		Samia	Guezane-Lakoud	
2		Meriem	Ferrah	
3		Mounia	Merabet-Khelassi	
4		Nourhane	Touil	
5		Martial	Toffano	
6		Louisa	Aribi-Zouioueche	

Response by Author: "Ok"

2. **Query** [AQ1] : Please check and confirm the surname and forname for all the authors and particularly for 'Samia Guezane-Lakoud'.
Response by Author: "Ok"

3. **Query** [AQ2] : Please check and confirm the inserted city and country name for the affiliation 'b'.
Response by Author: "Ok"

4. **Query** [AQ3] : Please provide complete details for (Rogova et al., 2021) in the reference list or delete the citation from the text.
Response by Author: "I delete the citation of (Rogova et al., 2021) from the text."

5. **Query** [AQ4] : Please check and confirm the edit made in the sentence 'Similarly, using toluidine with the above series …'.
Response by Author: "Ok"

6. **Query** [AQ5] : Please check and confirm the inserted citation for Table 7, and correct if necessary.
Response by Author: "Ok"

7. **Query** [AQ6] : No funding details have been found for your manuscript submission, so a Funding section has been added stating that no funding was received. Please correct if this is inaccurate.
Response by Author: "Ok"